

# SOIL MOISTURE RETRIEVAL ALGORITHMS USING SAR DATA

## A DISSERTATION

*Submitted in partial fulfillment of the  
requirements for the award of the degree  
of*

## INTEGRATED DUAL DEGREE

(Bachelor of Technology & Master of Technology)

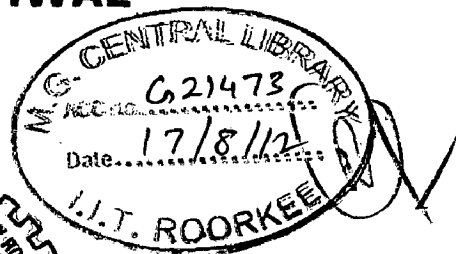
in

## ELECTRONICS & COMMUNICATION ENGINEERING

(With Specialization in Wireless Communication)

By

**LOKESH MEGHWAL**



DEPARTMENT OF ELECTRONICS AND COMPUTER ENGINEERING  
INDIAN INSTITUTE OF TECHNOLOGY ROORKEE  
ROORKEE - 247 667 (INDIA)  
JUNE, 2012

---

---

## CANDIDATE'S DECLARATION

---


---

I hereby declare that the work, which is being presented in this dissertation report, entitled "**Soil moisture retrieval algorithms using SAR data**" being submitted in partial fulfilment of the requirements for the award of the degree of Integrated Dual Degree (Bachelor of Technology and Master of Technology) in Electronics and Communication Engineering with Specialization in Wireless Communication, in the Department of Electronics and Computer Engineering, Indian Institute of Technology Roorkee (India), is an authentic record of my own work carried out under the guidance of Dr. Dharmendra Singh, Department of Electronics & Computer Engineering, Indian Institute of Technology, Roorkee.

The matter embodied in the dissertation report has not been submitted for the award of any other degree elsewhere.

Dated: 09/06/2012

Place: IIT Roorkee



**Lokesh Meghwal**

---

---

## CERTIFICATE

---

---

This is to certify that the above statement made by the candidate is correct to the best of my knowledge and belief. This is to certify that this dissertation entitled, "**Soil moisture retrieval algorithms using SAR data**," is an authentic record of candidate's own work carried out by him under my guidance and supervision. He has not submitted it for the award of any other degree.

Date: 09/06/12

Place: IIT Roorkee



**Dr. Dharmendra Singh**

Associate Professor

E&CE Department

IIT Roorkee

## ACKNOWLEDGEMENTS

It gives me great pleasure to take this opportunity and thank my guide Dr. Dharmendra Singh, Associate Professor, Department of Electronic and Computer Engineering, Indian Institute of Technology. Throughout the entire duration of thesis he has been an inspiration to me. He has constantly guided me academically and always motivated to always study hard. But he has not just provided help academically but also has been a mentor who gave encouragement and instilled motivation and gave a lot of encouragement to think creatively and develop an attitude of learning as much as one can. He is one of the best faculties I got to study from during my stay at IIT Roorkee.

I express sincere thanks to Dr.S.N.Sinha, Professor, Dr.Padam Kumar, Head of Department, Electronics and Computer Engineering, for providing for providing all the necessary facilities needed to carry out my dissertation. I thank I thank Dr.N.P.Pathak, Assistant Professor, Dr. M. V Kartikeyan, Professor, Dr. A.Patnaik, Assistant Professor, for their guidance, support and valuable teaching inside and outside the class.

I would like to thank all my lab partners for their valuable support. I would like to specially like to thank Ms.Pooja Mishra Mam for the valuable suggestions without which it would have been very difficult. I would like to thank Ms.Shivangi Goel for creating an atmosphere conducive of learning. I would like to thank Dr.Rishi Prakash for guiding me throughout my dissertation. I would like to thank my friend Jagannath Malik for his timely help on some topics.

I am thankful to the Ministry of Human Resource Development (MHRD) for providing financial help.

But above all I cannot forget to thank my parents, and my sister who has been a constant support throughout my life. I cannot imagine being able to achieve anything without their moral support.

Lokesh Meghwal

## ABSTRACT

The scattering of microwave radiation from soil surface are greatly affected by the local terrain as well as from different soil parameters. The dielectric property of soil being related to the soil moisture provides a good mean to find out the soil moisture. For this various researchers have developed many algorithms to exploit this feature of soil. However the SAR data available is not purely reflected from soil surface but also vegetation and other land cover classes. This challenge of discovering new techniques to normalize the effect of vegetation and find out the backscattering value only dependent on the soil surface requires normalizing vegetation effect. SAR data is a polarized data having different wavelength HH, VV, HV and VH. These wavelengths interact differently with different properties of soil from which we can use the best possible parameters that related to soil moisture.

But first the land cover is classified into various classes so as to identify different regions. From classification it can be seen that land belonging to same land cover class exhibits similar surface properties. So this classification is carried out using optical data. The optical data consists of spectral information of the class in visible region, infra-red and red region. And the spectral reflectance of surface is different for different land cover classes. Using this property of soil various indices are applied like the Normalized difference vegetation index (NDVI), enhanced vegetation index (EVI), Modified soil-adjusted vegetation index (MSAVI), Global environment monitoring index (GEMI), Purified adjusted vegetation index (PAVI) etc. are used. With the help of these indices various land cover are studied.

After classification the next main task done was estimating the soil moisture. Using the classified MODIS image the PALSAR image is superimposed in order to classify the PALSAR image. After classification the inversion approach is applied to the radar signal for estimating the soil moisture. In this thesis three inversion approaches are implemented, Bayesian approach, the neural network approach and an empirical approach. The result of the inversion is then checked out to find the limits of error on surface region. From this error estimation a minimum error limit is defined on received values from which surface regions having almost similar soil moisture can be classified into regions having similar moisture values.

<b>CANDIDATE'S DECLARATION.....</b>	<b>ii</b>
<b>LIST OF FIGURES.....</b>	<b>viii</b>
<b>LIST OF TABLES.....</b>	<b>x</b>
<b>Chapter 1.....</b>	<b>1</b>
<b>Introduction.....</b>	<b>1</b>
1.1. Objective of thesis.....	3
1.2. Problem statement.....	3
1.3. Organization of thesis.....	4
<b>Chapter 2.....</b>	<b>5</b>
<b>Brief literature review.....</b>	<b>5</b>
2.1. Microwave Remote Sensing.....	6
2.2. Satellite missions.....	7
2.3. Microwave Remote sensing.....	8
2.4. Passive Microwave theory.....	9
2.5. Active Microwave Theory.....	10
2.6. Satellite parameters.....	11
2.6.1. Frequency and Wavelength.....	11
2.6.2. Incidence angle.....	12
2.6.3. Polarization.....	13
2.7. Soil parameters.....	14
2.7.1. Dielectric constant.....	14
2.7.2. Surface Roughness.....	16
2.7.3. Soil texture.....	17
2.7.4. Topography of the region.....	18
2.7.5. Observation depth.....	19
2.7.6. Vegetation parameters.....	20
2.7.7. Normalized difference vegetation index NDVI.....	21

2.7.8. Leaf area index.....	22
<b>Chapter 3.....</b>	<b>25</b>
<b>Review of soil moisture retrieval models.....</b>	<b>25</b>
3.1. Theoretical models.....	25
3.2. Empirical Models.....	26
3.3. Semi empirical Backscattering models.....	28
3.4. Relationship between Moisture and backscattering coefficient.....	30
3.5. Effect of Vegetation on Soil Moisture Estimation.....	32
<b>Chapter 4.....</b>	<b>35</b>
<b>Study area and the data sets used.....</b>	<b>35</b>
4.1. PALSAR DATA.....	36
4.1.1. Preprocessing of PALSAR data.....	36
4.2. MODIS DATA.....	37
<b>Chapter 5.....</b>	<b>39</b>
<b>Methodology.....</b>	<b>39</b>
5.1. Methodology for Land cover classification using satellite data.....	39
5.2. Methodology for soil moisture estimation using satellite data.....	42
5.2.1. Steps to obtain SAR data normalized with respect to vegetation.....	43
5.2.2. Retrieval of soil moisture using various inversion approaches.....	47
5.2.2.1. Neural Network approach.....	47
5.2.2.2. Dubois model for soil moisture estimation.....	48
5.2.2.3. Nelder-Mead minimization method.....	50
<b>Chapter 6.....</b>	<b>53</b>
<b>Results and discussion.....</b>	<b>53</b>
6.1. Classification of image.....	53

6.2. Vegetation correction.....	59
6.3. Neural Network Approach.....	62
6.4. Nelder Mead Approach.....	68
<b>Chapter 7.....</b>	<b>71</b>
<b>Conclusion and future scope.....</b>	<b>71</b>
7.1. Conclusion.....	71
7.2. Future scope.....	73
<b>LIST OF PUBLICATION.....</b>	<b>75</b>
<b>REFERENCES.....</b>	<b>77</b>

## LIST OF FIGURES

Fig 1: Backscatter from forest area to L, C, and X band wavelength	12
Fig 2: Effect of incidence angle on backscatter from vegetation	13
Fig 3: Horizontal and vertical polarization	13
Fig 4: Backscattering values for different types of soil texture	17
Fig 5: Scattering of radiation from different surface texture	18
Fig 6: Difference in signal scattering due to topographic effect	19
Fig 7: Penetration depth depending on soil moisture content	20
Fig 8: Spectral response of vegetation	22
Fig 9: Backscattering of signal from soil as well as vegetation	29
Fig 10: Study region used for this thesis	35
Fig 11: Steps involved in preprocessing of PALSAR data	36
Fig 12: Steps involved in obtaining the backscattering coefficients from PALSAR	
Image	37
Fig 13: Finally applied decision tree on the MODIS image	41
Fig 14: Initial normalization of data with respect to vegetation	42
Fig 15: Neural network has an advantage that is little adaptive in nature.	48
Fig 16: Flow chart for Dubois Model	49
Fig 17: outline of Nelder-Mead minimization method	50
Fig 18: Raw MODIS Image	53



Fig 19: Image classified into different regions using various indices.	57
Fig 20: Comparison of growth for four months of (a) March, (b) April, (c) May, (d)June	58
Fig 21: Overall outline for vegetation correction	59
Fig 22: Relation between normalized HH with NDVI	61
Fig 23: Relation between normalized VV with NDVI	61
Fig 24: Whole process outflow for development of model for moisture calculation.	62
Fig 25: Comparison of mean absolute error with iterations for computing the soil moisture for bare soil	64
Fig 26: Iterations for training the data in vegetation region.	64
Fig 27: Histogram showing the frequency against errors.	65
Fig 28: Comparison of measured and estimated moisture values	66
Fig 29: Comparison of predicted and measured moisture values	66
Fig 30: Final moisture map generated by Neural Network Approach	67
Fig 31: comparison of result between measured and calculated soil moisture	68
Fig 32: Final moisture map generated by Nelder Mead Approach for same region as in Neural Network	69

## **LIST OF TABLES**

Table 1: Various bands in frequency spectrum	6
Table 2: Satellite missions that are presently active	7
Table 3: parameters used for designing neural network	48
Table 4: Final threshold values obtained for different vegetation contents	54
Table 5: Separability index obtained for different land cover classes	55

# Chapter 1

## Introduction

---

The top layer of earth crust known as soil bears a significance importance in our ecological system. The knowledge about its exact concentration equips us with a lot of information from which we can estimate different geological phenomena in advance. Soil parameters include its composition, texture, surface roughness, moisture content etc.

One of the important parameter of soil is the soil moisture. For our study purpose the considered soil moisture is mainly the moisture contained in the top 1-5cm thickness of soil as this is roughly the depth of penetration of Radar signal. The soil moisture is an important parameter for finding out about global climate changes and an important parameter for various ecological processes. From soil moisture information we can predict about the local topography, predicting its weather pattern, its soil fertility, floods and drought and thus becoming an important factor in crop yield.

But soil moisture varies with location to location. Because of the vastness the extraction of information about parameters of soil becomes a huge task which becomes extremely difficult to monitor. Going to every location and studying its various parameters is an extremely difficult and cumbersome take. So with this limitation various efforts were made to study the properties of soils remotely. Due to advancement of microwave remote sensing a lot of images and satellite data is available which helps in extracting the information and finding pattern in them.

Remote sensing simplifies the task of going to every location and one can estimate the exact information about soil to a great extent without actually going to the exact location. Various algorithms have been developed since past two decades which tries to find out relations between the parameters obtained from soil and the parameters obtained from satellite data. And from these algorithms developed its possible to find out properties of soil at each and every location.

Efforts to find out about soil moisture maps using microwave remote sensing has been in place as early as early as 1973[1]. Remote sensing mainly uses P, L, C and X bands.

Remote sensing can be classified into Active and Passive types. Passive remote sensing uses external sources which illuminate their targets and the signal reflected from that target is captured by the passive sensor. Active sensor has both the sensors, transmitting and as well as receiving. The signal is transmitted and then the scattered signal by the source is captured back.

Active systems are called as radar. Active radar systems offer many advantages as they use their own sensors and have the ability to penetrate clouds, smoke and moderate vegetation.

Many experimental campaigns have been conducted in the past decades which were used to find out about the soil moisture such as Washita 94 experiment. The experiment was conducted on watershed area of Oklahoma during 1994. Various ground visits were carried out to collect data and realize it SAR (synthetic aperture radar) perspective. The southern Great Plains experiment carried out in 1999(SPG99) was carried out to use data set from aircraft. Another experiment from sensors such as ASMR (advanced scanning ground microwave radiometer), Radar SAT, and various other aircraft remote sensing instruments were used.

Another important parameter is the surface roughness of the soil. This is an important phenomena and wind flow is the main reason of it. The rougher a surface is the more it blocks the wind flow. Surface roughness can be increased from the tillage operation that forms ridges and furrows and can bring clods to the surface. This smother the surface is the less the scattering occurs from the soil and thus less is the signal received back to the satellite.

Radar is classified into two types imaging and non-imaging radar, Canadian RadarSAT provides high resolution imaging while European ERS1 is non-imaging radar. The source is illuminated from the satellite signal which then gets scattered back and caught by the radar. This signal backscattered is called Radar backscatter ( $\sigma$ ). As this backscattered signal is reflected back from soil so it is dependent on satellite configuration such as incident angle( $\theta$ ) and also on soil properties such as dielectric constant( $\epsilon$ ), the roughness of the soil which is

measured in terms of rms height( $h$ ) of the soil, the correlation length ( $l$ ). The moisture of a soil can be most correlated to the dielectric constant of the soil. This dielectric constant is related to the composition of soil in terms of its clay, slit and sand present in the soil. So as this backscatter ( $\sigma$ ) value depends on the so many soil parameters from which soil moisture can be estimated. Its becomes a feasible solution to find out the various algorithms which defines function related to the estimation of soil moisture and radar backscatter ( $\sigma$ ). Various limitations are in terms of topographic variations, the low resolution (10mts to 1000mts) available in some cases and also the distortions provided by atmospheric factors such as clouds and smoke. The vast scale at which it operates is very large. Various techniques have been applied to tackle this problem by either taking multiple data with multiple combinations of polarization, incident angle and frequency.

### **1.1. Objective of thesis**

The objective of the thesis is to develop a model for estimating soil moisture which is adaptive in nature. That is it requires as little as possible apriori information about the surface in question. The models for moisture estimation are used for estimation using polarimetric SAR data and optical MODIS data available.

To estimate the moisture the model should take into consideration the vegetation effect of the land. The vegetation is an inherent part of land cover which interacts with the radar signal and thus obstructing the soil moisture estimation of the soil beneath it. The signal is transmitted by satellite is scattered from the surface. This signal is scattered from soil, vegetation, water bodies as well as manmade structures (urban region).

### **1.2. Problem statement**

So the work carried out in this thesis is summarized in following points.

- Application of satellite images for land cover classification, specially water, urban and agricultural classification.
- To study the various vegetation correction algorithms and implementation for soil moisture retrieval.

- Automatic generation of soil moisture map.

### **1.3. Organization of thesis**

In first chapter the objective and problem statements are given. Then in second chapter a brief literature overview of microwave radar remote sensing is given. This chapter deals about various aspects of active and passive remote sensing and also the soil as well as the vegetation parameters that effect the determination of soil moisture. In chapter 3 the review of already developed models on soil moisture retrieval are discussed and various theoretical, empirical and semi empirical models are developed. In chapter 4 the information about the data used is given and area location of study is mentioned. In chapter 5 the methodology used is explained and in chapter 6 the results and discussions are discussed. Finally conclusion and future scope are discussed.

# Chapter 2

## Brief literature review

---

Soil moisture estimation has always been an important area of study of remote sensing. Water is the most important resource for human kind as it is necessary to support all the life forms. Water estimation becomes more crucial due to its implications in various fields when its prior estimation can lead to proper planning in the areas of hydrological, agricultural, meteorological and climate. One of the main areas is agriculture. The knowledge about soil moisture helps in better judging the soil characteristics and helps in proper planning regarding crop planting and irrigation management.

The knowledge of soil moisture is important in terms of temporal and spatial terms. This estimates the evapo-transpiration, the energy is divided into two parts, latent heat energy and sensible heat energy [2]. The estimation of water budget in terms of the amount of water runoff and the amount of infiltration is necessary for judging the soil characteristics. All these information helps in estimating watershed modeling and that ultimately provides information on irrigation and hydroelectric capacity. In addition to economic advantage it also has sociological advantages also as it helps in estimation of various water borne diseases. It also helps in selecting suitable insecticides and pesticides depending on particular soil conditions. This knowledge about local and global soil moisture content is highly necessary in taking action for day to day activities [3].

Soil moisture measurement is dependent on various properties of soil. The dielectric constant of soil being one of the main factors and other factors being soil roughness, texture, vegetation etc.

The few basics of microwave engineering and radar basics are provided in the following section.

## 2.1. Microwave Remote Sensing

The microwave region is the region defined in the frequency spectrum from 0.3 to 300GHz. The various frequency bands that are divided in between are described in figure 1.1. The main advantage of using microwave region is because its ability to penetrate atmospheric aberrations such as clouds, smoke, rain, snow as well as a little amount of vegetation. Microwave radiations interact with different components of soil differently. And this electromagnetic signal is polarized and this interacts differently with bare soil, vegetation, urban and water. So this distinction in properties helps in studying about various properties of surface features separately and thus helps in classification as well estimation in study of different components of study.

BANDS	WAVELENGTH (cms)	FREQUENCY (GHz)
K <sub>a</sub>	0.75-1.18	40-26.5
K	1.19-1.67	26.5-18
K <sub>u</sub>	1.67-2.4	18-12.5
X	2.4-3.8	12.5-8
C	3.9-7.5	8-4
S	7.5-15.0	4-2
L	15.0-30.0	2-1
P	30.0-100	1-0.3

Table: 1 various bands in frequency spectrum

The microwave remote sensing systems can carry observe the target under all weather conditions this is not possible in the visible or infrared radiations. There are two types of microwave system Active and passive microwave systems. The passive microwave systems are dependent on the thermal emission of earth surface illuminated by sun. These thermal emissions are product of surface temperature and surface emissivity. On the other hand the active microwave systems are self-sufficient systems which carry their own radiating source. Hence they are not dependent on any external source. The active radiations emits the radiations towards the earth surface and the radiations which scattered back from the source comes back to the microwave system and thus it is called backscattering coefficient. The



backscattering coefficient consists of signal scattered not only from soil but also from vegetation as well as multiple reflection from soil and vegetation.

The resolution of space crafts has increased with time and in recent times a lot of fine resolution is available. The passive microwave sensors can have a good resolution of up to 100-1000mts. But the active sensors have a resolution up to 8mts (RADARSAT-1) and even better to 3mts (RADARSAT-2). This high resolution of data availability has improved the level of details available and thus the local effects can be more included in the techniques applied, thus providing with more accurate results.

## 2.2. Satellite missions

A lot of satellite missions have been carried out in the last three decades. The satellite missions such as FIFE(87-89), MANSOON(90), OXSOME(90), MACHYDRO(90), HAPEX(90-92), WASHITA(92), SGP(97), SGP(99), SMOSREX(01-06), SMEX(02), SMEX(03), and SMEX(04) were carried out to find out about soil properties[3-8].The currently active satellite programs as follows [9]

System/ Instrument	Country	Owner/Operator	Prime	Launch Date(s)	Orbit Altitude (km)	Repeat Cycle (days)
QuikScat/ Seawinds	USA	NASA	JPL	Jun-99	803	
TRMM	USA, Japan	NASA, JAXA	GSFC	Nov-97	402.5	
Cassini	USA, Italy	NASA	JPL	Oct-97	(Saturn/ Titan)	
Cloudsat	USA	NASA	JPL	Apr-06	705	
JASON-1/ Poseidon-2	USA, France	NASA, CNES	Alcatel	Dec-01	1336	10
MRO/ SHARAD	USA, Italy	NASA	JPL	Aug-05	(Mars)	
Radarsat-1	Canada	CSA	Spar Aerospace	Nov-95	798	24
Mars Express/ MARSIS	ESA, USA, Italy	ESA/ASI/NASA	Alenia/JPL	Jun-03	(Mars)	
ERS-2	ESA	ESA	EADS Astrium	Apr-95	800	35
ENVISAT	ESA	ESA	EADS Astrium	Mar-02	800	35
SAR Lupe	Germany	BMVg	OHB System	Dec-07	500	NR
ALOS/ PALSAR	Japan	JAXA	NEC, Toshiba, MELCO	Jan-06	692	46
IGS	Japan	MOD	MELCO	Mar-07	NR	NR

Table 2: Satellite missions that are presently active [9]

### **2.3. Microwave Remote sensing**

Microwaves are electromagnetic waves with wavelengths ranging from 1m to 1mm, with frequency between 0.1GHz and 300GHz. The most important reason for using microwaves for remote sensing is their capability to penetrate clouds and also rain and their independence of sun as a source of illumination. Another reason is that they are able to penetrate more deeply into vegetation than optical waves [3].

Various satellites like (ERS-1, ERS-2, SIR-C/X-SAR, JERS-1 and RADARSAT-1, ENVISAT, ALOS/PALSAR) provide data which is highly useful in estimating soil moisture of roughly top 5cms of soil layer. The spatial and temporal variations of soil moisture are clearly defined for each point location. The satellite images being remotely taken are affected by the soil characteristics such as surface roughness, texture, vegetation (leaf area index, vegetation water content, density of vegetation, vegetation height etc.).

So the main focus becomes to also account for these local topographic effects when the soil moisture estimation is done. The urban and water regions are classified and removed for calculation purposes.

The main frequency used for studying satellite images is the C (4-8 GHz) band and L (1-2 GHz) band. The reason for using these bands is their capacity to penetrate through the atmospheric and surface aberrations like clouds, smoke and mild vegetation. Among these the C band gives good results in shallow and mild vegetation and agricultural regions with small height vegetation. And L band is preferred tall vegetation like forest.

But the vegetation estimation is better done using the optical sensors. The various frequency bands from 620-2155nm show good correlation with vegetation cover, water as well as building structure. Different indices like NDVI, EVI etc. are highly correlated to vegetation cover thus giving a relation between vegetation and satellite data. This data can further be complimented with the microwave data to get better estimation of soil properties in the regions where there is vegetation [9].

The microwave remote sensing is very popular because of the application of the soil moisture and various other parameter estimation remotely without even being in the contact of the

target. The point to point observation is very difficult for such vast scale as land surface. For this the regions of the earth surface are studied using both active and passive sensors and are used to measure soil moisture. The microwave is preferred over other electromagnetic radiations because of its ability to penetrate various other targets such as smoke, cloud and in some cases small vegetation also [11].

The microwave is classified into two categories Active and Passive. Active sensors are the sensors which have both transmitting and receiving source while passive sources have only receiver and they are dependent on other sources for their illumination. The soil moisture estimation depends on various factors. Some of these are satellite factors and some of these are the soil properties. In this section these are discussed in detail. First the two types of microwave imaging Active and Passive are discussed and then the soil properties which effect the estimation of soil moisture are discussed.

#### **2.4. Passive Microwave theory**

The principle of passive remote sensing is as already mentioned above is dependent on the illumination of the source by external source which may be sun or some other signal source. The passive sensors generally measure the natural thermal emission of the land surface at microwave wavelength. The microwave brightness is a function of the thermodynamics of the soil temperature and emissivity. The relation can be defined in the following equation

$$T_B = R \cdot \tau \cdot T_{sky} + (1 - R) \cdot \tau \cdot T_{soil} + T_{atm} \quad (2.1)$$

Where R = surface reflectivity,

$\tau$  = atmospheric transmissivity,

$T_{sky}$  = contribution from the reflected sky brightness,

$T_{soil}$  = thermometric temperature of the soil,

and  $T_{atm}$  = is the average thermometric temperature of the atmosphere.

The surface emissivity ( $\epsilon_s$ ) can be approximately calculated by dividing brightness temperature ( $T_B$ ) by soil surface temperature (TS).

The passive microwave response which is the surface brightness decreases with the increasing soil moisture which is just reverse with that found in active microwave sensing [7].

At longer wavelengths of greater than 10cms the atmospheric transmission is about 99% and the  $T_{atm}$  and  $T_{sky}$  contributions are less than 5° K. when this happens the second term becomes the major contributor for surface brightness and this is related to the surface moisture and surface roughness. For bare soil the measured temperature is directly related to the soil water content and the temperature of the soil.

The vegetation emits its own microwave radiation and this energy interacts with the energy emitted by the soil. This energy may increase or attenuated depending on the vegetation characteristics. Various models have been developed to estimate soil moisture under the vegetation cover by [7, 9]. But as the aim of this thesis is to study the effects of soil moisture on active sensors satellites so active microwave remote sensing is given in detail.

## 2.5. Active Microwave Theory

Active microwave systems generate their own radiation transmitted towards earth surface and measure the returning radiation. The ratio of strength of received and transmitted signal (backscattering coefficient) depends on surface reflectivity and the antenna characteristics such as incidence angle, wavelength, and polarization. This coefficient is the average value of the scattering cross-section per unit area, “the amount of energy that is scattered back to the receiving sensor per unit area”. The strength of backscattered signal (backscatter coefficient or sigma naught,  $\sigma_o$ ) is usually expressed in decibels using a logarithmic scale because of the large dynamic range of its values. The relationship between backscattering coefficient and other radar parameters is given by radar equation [7]

$$\sigma^0 = \frac{P_r (4\pi)^3 R_r^4}{P_t G_t G_r \lambda^2 A} \quad (2.2)$$

Where,

$\sigma_0$  = Backscatter coefficient

$P_r$  and  $P_t$  = received and transmitted power,

$G_r$  and  $G_t$  = received and transmitted antenna gain,

$\lambda$  = wavelength,

$R_t$  = target range

$A$  = target area

The most widely used active remote sensing systems are: RADAR (Radio Detection And Ranging), LIDAR (Light Detection And Ranging), and SONAR (SOund Navigation And Ranging). The radar images are obtained from aircraft or spacecraft using the continuous-strip mapping capability of side-looking radar (SLAR). The SLAR is classified in two types: real aperture radar (RAR) and synthetic aperture radar (SAR).

The radar spatial resolution is a function of the pulse length and the antenna beam width, which is governed by the length of the antenna. Thus, finer spatial resolution is obtained by increasing the length of the antenna. For example, 10 m resolution requires a 4 km long antenna. Therefore, to produce the desired resolution, the SAR system uses forward motion of the spacecraft to synthesize a much longer antenna to generate high resolution images even from space. The antenna length is simulated by appropriate processing of a large number of return signals along the flight trajectory [10].

## **2.6. Satellite parameters**

### **2.6.1. Frequency and Wavelength**

The frequency of incident radiation has a direct relationship with the penetration depth in the surface and the relative roughness of the surface. The penetration depth is a function of surface roughness and relative roughness of soil. The L band penetrates higher into

vegetation. The Cloud penetration of C-band is highest and that of X-band is least. This can be seen in the figures shown below.

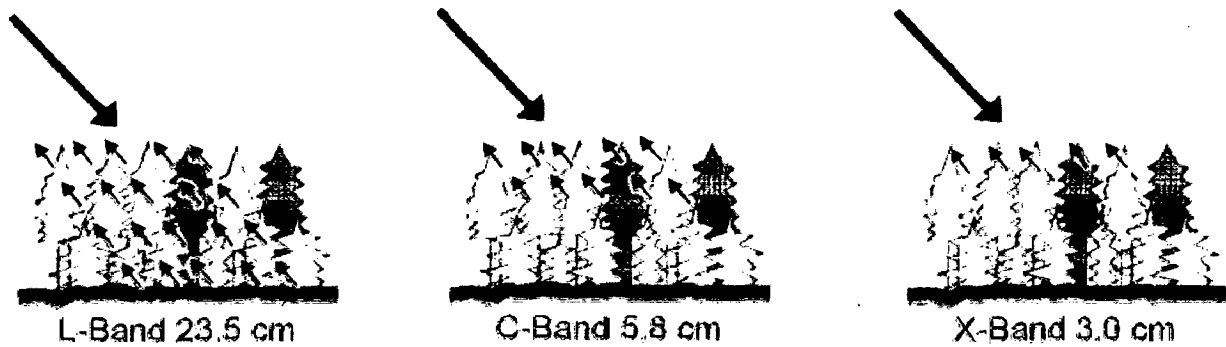


Fig 1: Backscatter from forest area to L, C, and X band wavelength [24]

The main aim in this thesis is to study the soil moisture with proper account of penetration and reflection from trees. In sparse vegetation, L band interacts more with underlying surface rather than vegetation, reducing its sensitivity to vegetation [24]. The penetration depth of the radar signal is a function of the frequency and moisture content of soil. The reflection is mainly observed from a fixed angle so the factor of reflection is dependent on the polarization [25].

### 2.6.2. Incidence angle

The incidence angle ( $\theta$ ) is the angle between radiation direction and the surface as shown in fig 2. The incidence angle is a relation between the surface layer and the satellite position. The incidence angle changes across the radar image swath for the same image from near end to far end. The radar backscatter causes variations in the backscattered values obtained.

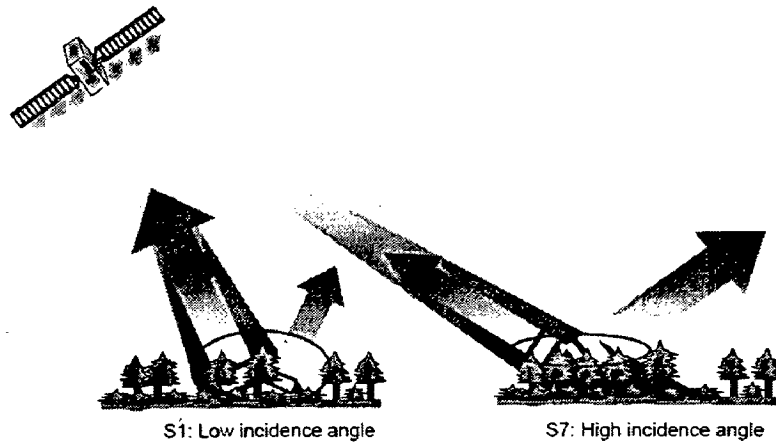


Fig 2: Effect of incidence angle on backscatter from vegetation [20]

### 2.6.3. Polarization

The EM radiations travel in two ways as horizontally and vertically. The two polarizations are termed as H polarization and V polarization (Fig 3). This polarization provides an important feature to estimate the moisture of the soil because the two polarizations interact with vegetation and soil differently. The Radiations transmitted and received are of the following configurations as HH and VV. And also the cross polarizations such as HV and VH. The first term is the transmitted term and the second term is the received term. The cross polarization terms are same. So any one value of HV or VH is considered.

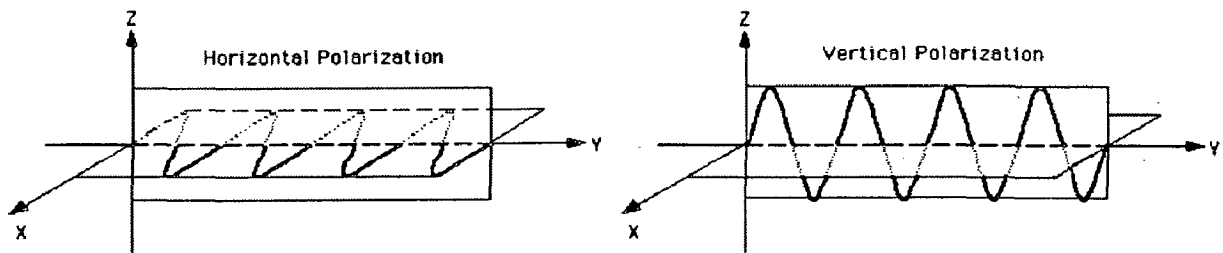


Fig 3: Horizontal and vertical polarization

Other important values that are considered are the differences between the cross polarization differences. The value of the differences is as shown below:

$$\text{Co-polarized phase difference: } \Phi_C = \Phi_{HH} - \Phi_{VV} \quad (2.3)$$

$$\text{Cross-polarized phase difference: } \Phi_X = \Phi_{HV} - \Phi_{VV} \quad (2.4)$$

This co-polarized phase difference is an important term found in the application of various processes. Various other difference terms are also considered which are used to produce five different phase products  $\Phi_{HH}$ ,  $\Phi_{VV}$ ,  $\Phi_{HV}$ ,  $\Phi_C$ , and  $\Phi_X$  [48].

Different polarizations can have different penetration depths for the same frequency and the soil dielectric constant. These polarization configurations are used to retrieve more accurate information from different layers of the target surface [13]. For example, for the same soil and land cover conditions. The VV and HV polarization are very sensitive to the incidence angle. VV polarization has higher penetration depth than HH polarization. While the effect of incidence angle on backscattering coefficient for HH polarization is weaker than VV and HV polarization [13]. At L-band, the polarization is dominant on scattering mechanism. VV polarization is more sensitive to the vegetation backscatter. Ground penetration and values reflected are comparable in response to the vegetation backscatter. These values are termed in terms of horizontal to vertical cross polarization and VV polarization. An index is given by for calculating the vegetation index as (SBVI) as follows: [23]

$$SBVI = \frac{\sigma_{L-HV}}{\sigma_{L-VV}} \quad (2.5)$$

The need of multi-polarization and multi-frequency SAR information is required for accurate retrieval of soil moisture from vegetated and roughly surface area [14]. So overall conclusion is that the multipolarisation helps in finding out the vegetation and bare soil moisture content.

## 2.7. Soil parameters

### 2.7.1. Dielectric constant

The Remotes sensing is based on sensing the electromagnetic signal that is send to the surface and then analyzing the signal received back. This signal responds differently to the soil properties, soil moisture being one of them. The reason that the soil moisture is able to produce change in the signal send back is because of the signal being changed on interacting with the water molecules present in the soil. The reason this happens is because of the water



molecules are dielectric in nature microwave signal interacts differently it compare to a bare soil. And soil moisture is a function of the dielectric constant of the soil. This relationship happens because of the contrast in properties of soil moisture and with dry soil. So the soil moisture value changes the dielectric constant of soil. The dielectric constant is also dependent on various other properties of soil such as soil texture, salinity, organic matter, bulk density and also temperature. But the major effect of change produced in dielectric produced in soil is due to the soil moisture. The increase in soil moisture is a function of increase in dielectric constant [10]. The dielectric constant is generally related to the soil moisture with a polynomial curve fitting relation.

The dielectric constant is not a simple numerical quantity but a complex entity having real and imaginary parts as shown in equation (1)

$$\varepsilon = \varepsilon' + j\varepsilon'' \quad (2.6)$$

The real part is actually the relative permittivity of the material with the respect to unity and the imaginary part represents the lossless part. The dielectric values of soil and water vary very much by almost an order of 20 at 1GHz [10].

For expressing the relation of soil moisture with dielectric constant the following relation as shown in (2) was derived [7].

$$\varepsilon = 1 + \frac{\rho_b}{\rho_{ss}} (\varepsilon_{ss} - 1) + m_v^{\beta} (\varepsilon_{fw} - 1) \quad (2.7)$$

Where

$\rho_b$  = bulk density,  $\rho_{ss}$  = solid material,  $\varepsilon_{ss}$  = dielectric constant of materials

$m_v^{\beta}$  = volumetric moisture of soil,  $\varepsilon_{fw}$  = dielectric constant of freewater

The vegetation is approximated as dry vegetation mixed with components of bound water and free water [10].

$$\varepsilon_{veg} = \varepsilon_r \varepsilon_{bd} \cdot v_{bd} + \varepsilon_f \cdot v_f \quad (2.8)$$

Here  $v_f$  = freewater,  $v_{bd}$  = boundwater

This vegetation dielectric constant is then using the above relation is found out using the following relation

$$\epsilon_{canopy} = [1 + v_f(\epsilon_{veg} - 1)]^{\frac{1}{\beta}} \quad (2.9)$$

Here the value of  $\beta$  is 0.5 for refractive model and 1 for linear mode. The value of  $v_f$  is called as volume fraction[11].

### 2.7.2. Surface Roughness

In simple words the surface roughness can be defined as the smoothness of soil. It is the irregularities of the surface. The roughness has a huge effect on the radar backscatter as the rougher the surface is the more are the radio signals transmitted in all the directions. Completely smooth surface like that of water scatters no radiation back to the satellite and hence no signal is received from it back. Vegetation on the other hand is very smooth and hence can be considered as rough. But the degree of roughness is relative to the signal used by the satellite. If an L band signal (wavelength=21cms) is sent then the surface might be smooth for it but it may be rough for C band (wavelength=5cms). So a mathematical relation shown in (5) to judge whether a surface is smooth or rough.

The surface is rough if it satisfies the following relation

$$h < \frac{\lambda}{8 * \cos\theta} \quad (2.10)$$

And it is rough if

$$h > \frac{\lambda}{8 * \cos\theta} \quad (2.11)$$

Where

$h$ =mean height of surface variations,

$\lambda$  = wavelength

and  $\theta$  = incidence angle

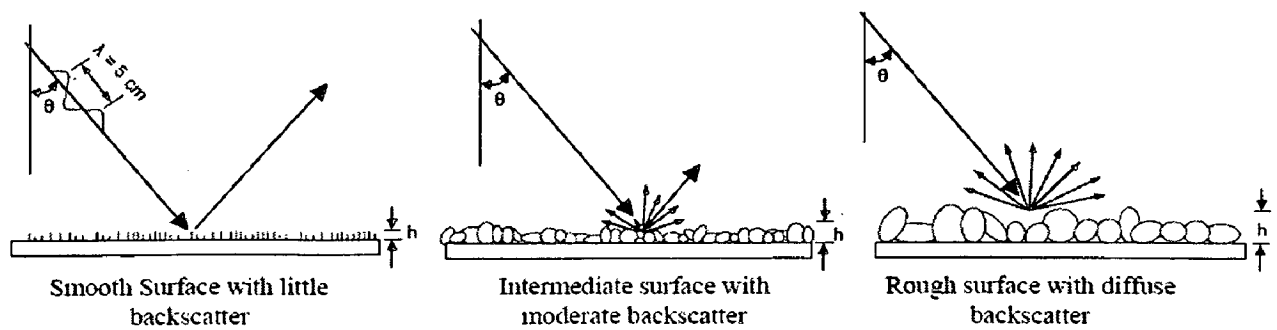


Fig 4: Backscattering values for different types of soil texture [20]

So water bodies are very smooth to almost all the incident wavelengths hence they don't reflect back any signal back to satellite. Other surfaces like forest are very rough and thus they scatter very less signal back to the satellite. While there are intermediate surfaces like bare lands and farms which scatter an intermediate signal back to satellite. This property of different scattering can lead to classification of surfaces into different classes.

### 2.7.3. Soil texture

Soil texture is related to the composition to the three major classes such as sand, silt and clay. And this is dependent on the moisture of soil. Soil moisture can be directly correlated to the dielectric constant of the soil. This relation can be seen from figure 2. As seen from the above figure that the values of backscatter are higher for the increasing clay concentration in soil. The more is the water content in the soil; more is the clay concentration in the soil. From above figure it can be seen that clay soil has the property of holding more water, which can be related to higher dielectric values of clay [11]. This can be then related to the further dielectric nature of water. The drier the soil is, the lower is the water content and hence lower is the clay concentration and hence lower is the backscattering value of the signal reflected back to the satellite.

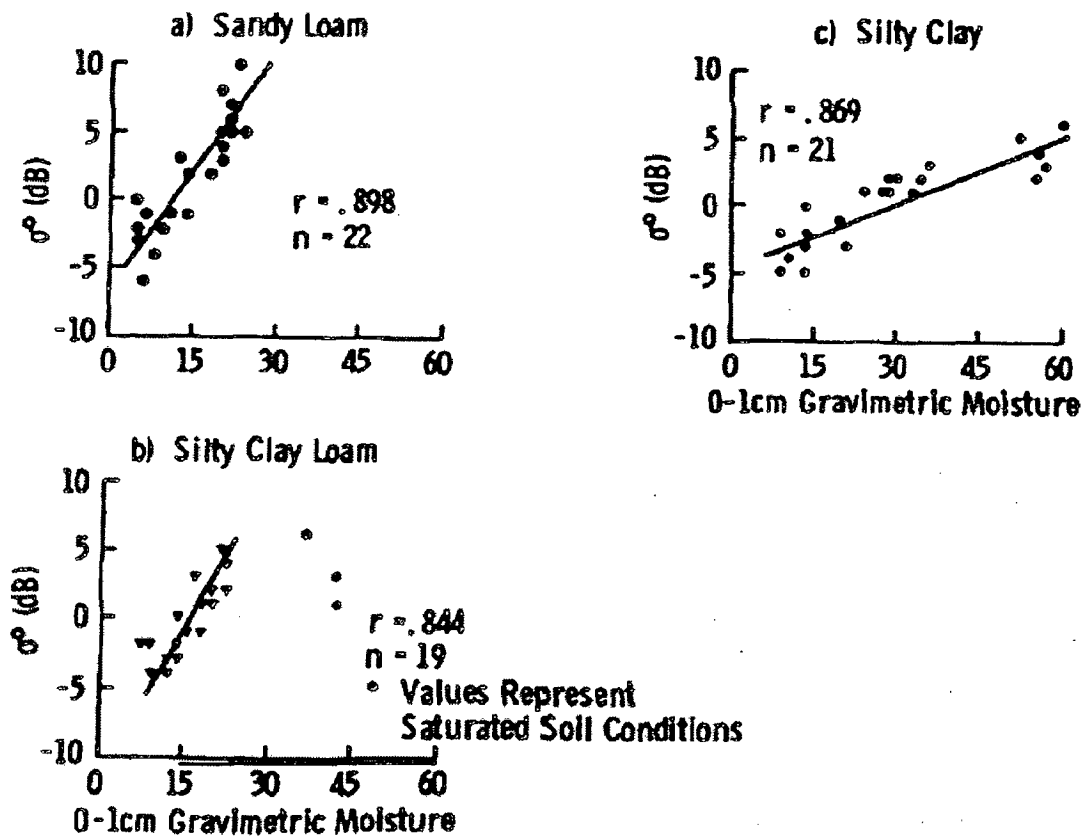


Fig 5: Scattering of radiation from different surface texture [11]

#### 2.7.4. Topography of the region

The topography relates to the relative orientation of satellite signal with respect to the land inclination. The local incidence angle is dependent on the surface inclination. This variation in topography leads to difference in backscattering of signal from the two surfaces. The surface facing the satellite is more capable of reflecting the signal and the surface lying opposite to the satellite is less capable of reflecting back the signal [12]. This can be seen from the figure 3

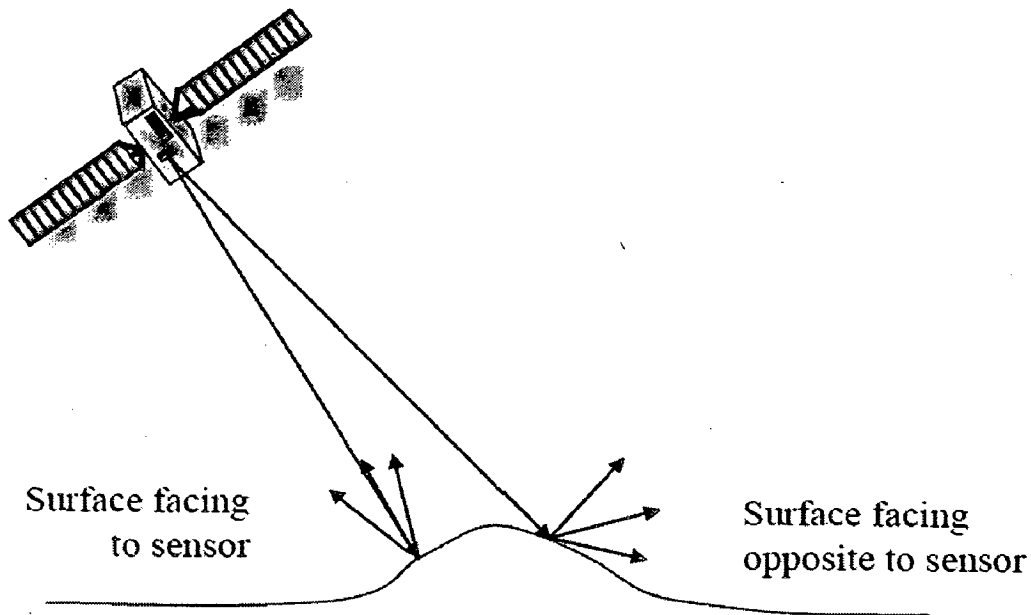


Fig 6: Difference in signal scattering due to topographic effect [20]

This effect is more comes into picture when the satellite is studying the mountainous region. The HH component of the polarized signal is more affected by topographic effects. The topographic effect produces errors in signal for values less than 1dB for lower topographic variations and it produces an error of values 5dB or more for surfaces with large variations [13].

To overcome this problem of topography a digital elevation model (DEM) is taken into account and it is given by following relation given in equation 2.12. [7]

$$\cos \vartheta = \cos S * \cos Z + \sin S * \sin Z * \cos(T - A) \quad (2.12)$$

Here  $\vartheta$  = incidence angle in degree,

S=the slope of pixels in degree,

Z=zenith angle of the sensor,

A=aspect angle of the pixel position (degrees) [14]

### 2.7.5. Observation depth

The penetration of the radar signal into the soil is dependent on the properties of soil, frequency of signal used and also on the radar polarization. The depth of the radiation penetrated in the ground is also dependent on the surface soil moisture. It decreases with the increase in soil moisture. This can be seen in the fig4 shown below. The penetration is

dependent on the dielectric properties of soil. The higher the dielectric constant the lower is the penetration depth. The polarization also affects the penetration depth. With the VV polarization the signal penetrates more the HH polarization. The dependence of penetration can be seen from the following figure.

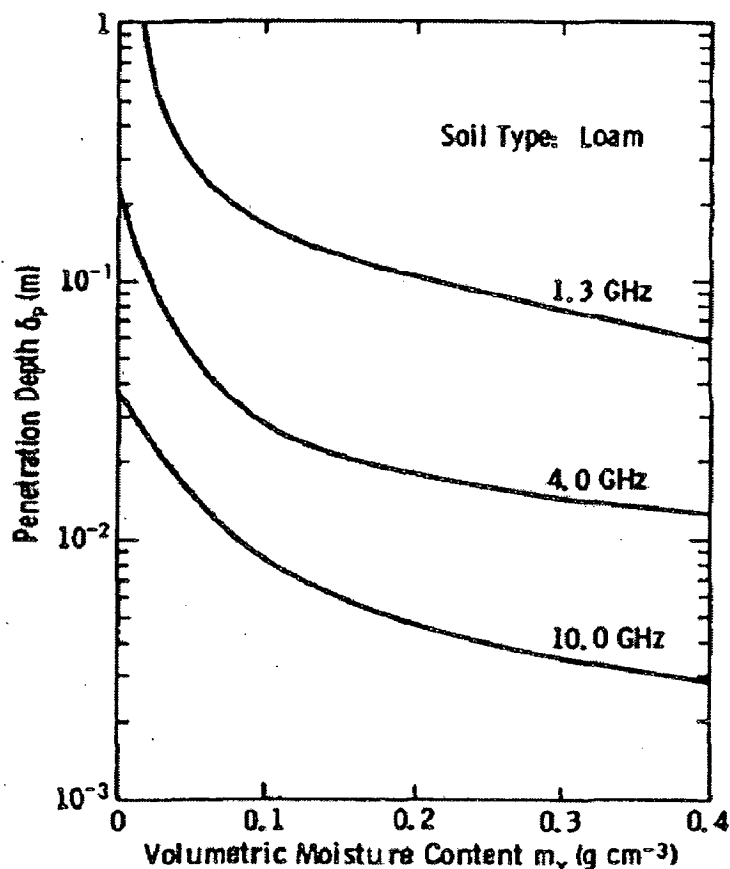


Fig 7: Penetration depth depending on soil moisture content [7]

### 2.7.6. Vegetation parameters

Vegetation cover is an important parameter in the detection of radar backscatter. The vegetation is very rough and also the radar signal interacts differently with the respective polarization. The degree of interaction of the radar signal with the soil moisture depends on the properties of soil cover. The polarization also comes into picture. Due to the contrast in the interaction of radar signal with the vegetation cover various indices are developed for studying the vegetation cover.

The vegetation cover is generally observed in the optical range. The region is studied in the optical range and then the values are used to find the vegetation indices. Then these values are then superimposed on the other microwave data available. Then from this vegetation cover is normalized with respect to bare soil and then the whole region is studied as bare soil.

The following section explains about some of these vegetation indices.

### **2.7.7. Normalized difference vegetation index NDVI**

The most common vegetation indices that are taken as Normalized difference vegetative index. The difference in the spectral behavior of vegetation with optical signal is used to find out the vegetation index. The vegetation is dependent on the process of photosynthesis for which it absorbs light. The plants generally absorb the visible spectrum of the light which is the blue and red and strongly reflect the near infra-red part of the signal. The green leaves of the plant and trees absorb the visible light and the mesophyll cell reflects the light in near-infrared wavelengths. But this whole process is only dependent on the photosynthesis process of absorption and reflection which is absent in other regions of bare soil, water, snow, and urban region. So this property is used to normalize the vegetation cover of the region. The spectral response of the vegetation is seen in the following figure.8

This NDVI can be mathematically defined as the difference between the near infrared and red divided by the summation of near infrared and red. This is represented in the following formulae of (8)

$$NDVI = \frac{NIR - RED}{NIR + RED} \quad (2.13)$$

The values of NDVI from the formula can be seen that lies between -1 to +1. With negative values representing no reflectance which comes from water and sometimes from urban region. While positive values represent the effect of vegetation.

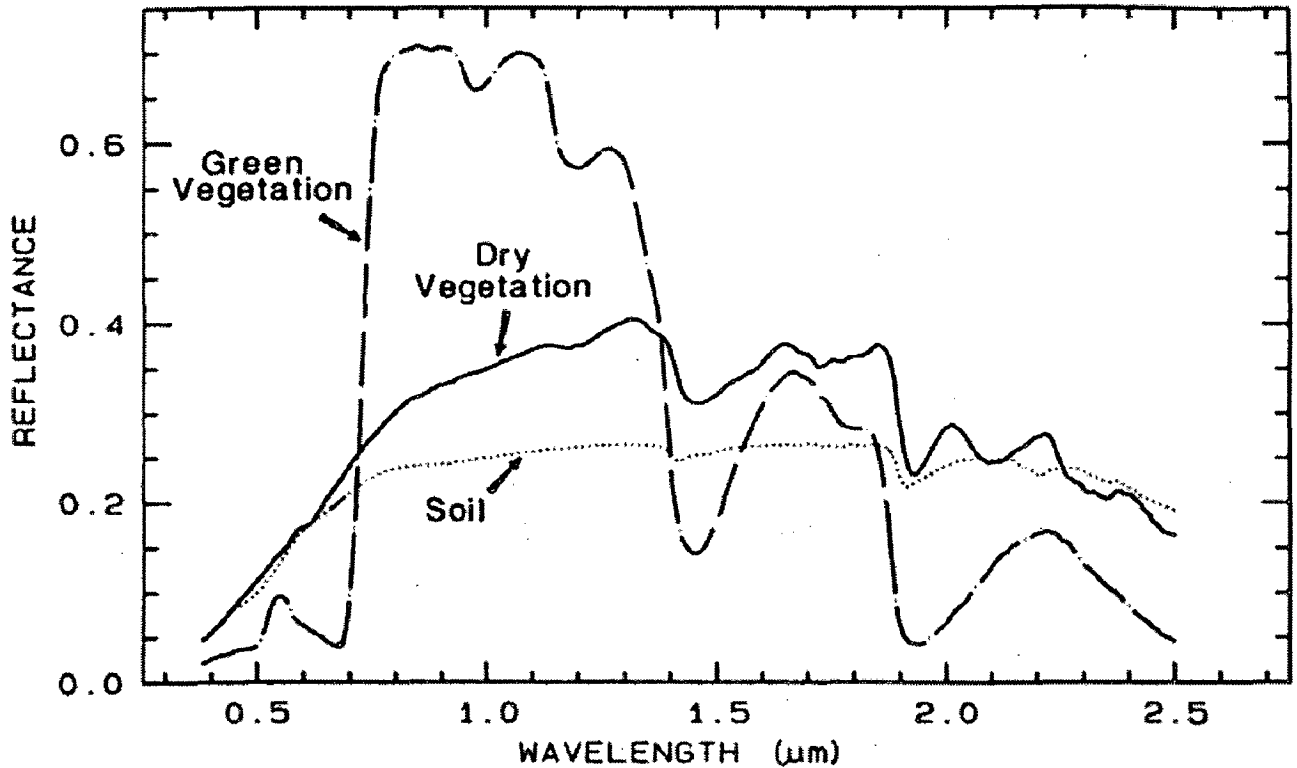


Fig 8: Spectral response of vegetation [7]

The values close to 0 represent bare soil while the values higher than 0.2-0.3 represent the presence of vegetation. Values higher than 0.5 is used to represent good vegetation areas. There are many regression relations existing between finding NDVI from the polarization of the radar signals. The cross polarization ratios for L band data and NDVI generated by another relation between was established the relation between NDVI and soil moisture content. Although it's not exactly relation and it's a crude approximation but still the NDVI values respond to the change of soil moisture at different depths of vegetation. [15].

### 2.7.8. Leaf area index

LAI is approximated with the values of density of vegetation in a region. This is a dominant variable among the estimation of vegetation using the process of photosynthesis, the transpiration, the energy balance and also the hydrological and ecological modeling. The LAI



value is dimensionless quantity varying from 0 to 16 describing the number of leaf layers plant canopy. The relation of the formulae for leaf area index is given below.

$$LAI = \frac{\text{leaf area (m}^2\text{)}}{\text{surface area (m}^2\text{)}} \quad (2.14)$$

The values equal to 0 indicates no leaves and values close to 1 indicate leaf area equal to actual area under observation. The value of LAI equal to 2 represents the volume of vegetation is double the area under observation. And the maximum value of 16 represents a very dense concentration of vegetation value.

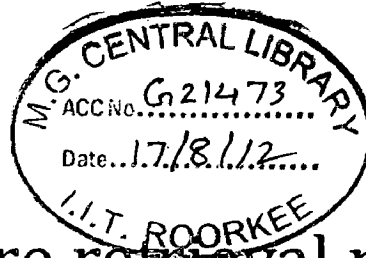
The measurement of LAI is done by two methods. Direct method and Indirect method. The direct method is very cumbersome and requires the estimation of plant values in a particular dimension of area. The values in direct estimation includes the area of harvest, the leaf litterfall and allometry equations. The indirect method involves the use of photometer to judge the light transmission.

The values obtained using NDVI are related to the LAI. The detailed relations between NDVI and LAI are tried to setup. Some results were given by [46]. The relationship of LAI can be setup from the NDVI values. From considering a relationship given by [16] is given below.

$$LAI_i = LAI_{max} * \frac{NDVI_i - NDVI_{min}}{NDVI_{max} - NDVI_{min}} \quad (2.15)$$

Here the values of  $i$  represents the maximum and minimum period for which it is observed. The maximum and minimum values of NDVI are sometimes obtained using multi-temporal images.





# Chapter 3

## Review of soil moisture retrieval models

---

As a large amount of satellite data is available which depends on the relation of soil moisture with backscattering values with different polarization. Many models have been developed by people to calculate soil moisture and various approaches have already been in place to find a proper relation to get the estimate to of soil moisture. Various theoretical and empirical relations are already developed. Some semi-empirical relations are also developed to find out about the moisture. Some of the theoretical models such as developed by [17].and empirical models [18-19] have become the basic models on which improvements have been done from time to time to get better and better results. The theoretical models were based on study of interaction of radar signal with the scattering of signal. Various parameters like frequency, polarization and incidence angle were taken into account and various surface characteristics were obtained from them.

Some of these models are briefly discussed in the following sections:

### 3.1. Theoretical models

In 1992 Fung et al [20] developed an IEM (integration equation model) based on electromagnetic spectrum model for bare soil surface. The details of which are given below.

$$\sigma_{pp}^0(\theta) = \frac{k^2}{2} e^{-2k^2 h^2 \cos^2 \theta} * \sum_{n=1}^{\infty} f_n^{2n} \frac{|I_{pp}^n|^2}{n!} W^{(n)}(-2k_v, 0) \quad (3.1)$$

$$\text{Where, } I_{pp}^n = (2k \cos \theta)^n f_{pp} * e^{-k^2 h^2 \cos^2 \theta} + \frac{(k \cos \theta)^n}{2} F_{pp} \quad (3.2)$$

$$f_{vv} = \frac{2R_{\parallel}}{\cos \theta} \quad f_{hh} = -\frac{2R_{\perp}}{\cos \theta} \quad (3.3)$$

$$F_w = \frac{2 \sin^2 \theta}{\cos \theta} \left[ \left( 1 - \frac{\epsilon \cos^2 \theta}{\epsilon - \sin^2 \theta} \right) (1 - R_{\parallel})^2 + \left( 1 - \frac{1}{\epsilon} \right) (1 + R_{\parallel})^2 \right] \quad (3.4)$$

$$F_{hh} = \frac{2 \sin^2 \theta}{\cos \theta} \left[ 4R_{\perp} - \left( 1 - \frac{1}{\epsilon} \right) (1 + R_{\perp})^2 \right] \quad (3.5)$$

$$W^n(k_x, k_y) = \frac{1}{2\pi} \iint \rho^n(\tau_x, \tau_y) e^{-j(k_x \tau_x + k_y \tau_y)} d\tau_x d\tau_y$$

$$h^2 \rho(\tau_x, \tau_y) = \langle Z(x, y) * Z(x + \tau_x, y + \tau_y) \rangle \quad (3.6)$$

Where,  $pp = hh$  or  $vv$ ,

$k$  = wave number of medium 1.

$k_s = k \sin \theta$ .

$h$  = rms surface height,

$\theta$  = incidence angle,

$\epsilon$  = dielectric constant of the surface,

$R_{\parallel}$  = Fresnel reflection coefficient for vertical polarization,

$R_{\perp}$  = Fresnel reflection coefficient for horizontal polarization,

$W^n(k_x, k_y)$  = Fourier Transform of the  $n^{\text{th}}$  power of the surface correlation coefficient,

$Z(x, y)$  = surface function, a stationary random process with zero mean, and

$\langle \rangle$  denotes the ensemble average operator.

But this method of IEM was a quite complex which was simplified as given in [19]. To predict the value of moisture of soil even in vegetation region, regression was done to estimate the relation of soil moisture between the various soil parameters as well as sensor parameters. This IEM model was then tested and modified by many researchers to find out relations between soil moisture and surface properties [18, 19, 20, 21, and 22].

### 3.2. Empirical Models

Various empirical models were also developed which used the value of satellite as well soil properties and relation was found out. One of the first attempts was proposed to develop a relation between the co-polarized and cross-polarized backscattered values. The model was given by [18]. The model is given below.

$$\sigma_{hh}^0(\theta, \epsilon_r, ks) = g \sqrt{p} \cos^3 \theta [\Gamma_v(\theta) + \Gamma_h(\theta)] \quad (3.7)$$

$$\sigma_{vv}^0(\theta, \epsilon_r, ks) = \frac{g \cos^3 \theta}{\sqrt{p}} [\Gamma_v(\theta) + \Gamma_h(\theta)] \quad (3.8)$$

Where

$$\begin{aligned}
 \varepsilon_r &= \text{real part of the dielectric constant}, \\
 s &= \text{rms height of surface}, \\
 g &= 0.7[1 - \exp(-0.65(ks)^{1.3})] \\
 \sqrt{p} &\hat{=} \sqrt{\frac{\sigma_{hh}^0}{\sigma_{vv}^0}} = 1 - \left(\frac{2\theta}{\pi}\right)^{[1/\Gamma_0]} * e^{-ks}, \text{ and}
 \end{aligned} \tag{3.9}$$

$$\text{Fresnel reflectivity of the surface at nadir, } \Gamma_0 = \left| \frac{1 - \sqrt{\varepsilon_r}}{1 + \sqrt{\varepsilon_r}} \right|^2$$

The applicability was further tested with various modifications by [20]. The linear regression was developed as shown below

$$\ln(M_v) = C_1 * \sigma_{(hh/vv)}^0 + C_2 * \theta + C_3 * f + C_4 \tag{3.10}$$

Where

$$C_1 = -0.09544, C_2 = -0.00971, C_3 = 0.029238, C_4 = -1.74678. \tag{3.11}$$

The values of backscatter are in dB and incidence angle in degrees, the frequency is put in GHz and the C4 is an offset constant value.

Dubois et al (1995) [23] used a ground measurements using ground based scatterometer. The model derived a relation between the bare soil backscattering coefficient and the dielectric constant of the soil. The parameter which he used for the calculation of soil moistures were as follows calculates the backscatter coefficient of bare surface as function of dielectric constant, surface roughness range= 0.3-3 cm

Incidence angle range= 30-65°

and frequency (range 1.5–11 GHz).

The relation between the backscattering in HH and VV polarize cross-sections derived as:

$$\sigma_{hh}^0 = 10^{-2.75} \frac{\cos^{1.5} \theta}{\sin \theta^5} 10^{0.028\varepsilon \tan \theta} (ks \sin^{1.4} \theta) \lambda^{0.7} \tag{3.12}$$

$$\sigma_{vv}^0 = 10^{-2.75} \frac{\cos^3 \theta}{\sin \theta^5} 10^{0.046\varepsilon \tan \theta} (ks \sin^3 \theta)^{1.1} \lambda^{0.7} \tag{3.13}$$

$\theta$  is the incidence angle,

$\varepsilon$  is the real part of the dielectric constant,

$S$  is the RMS height of the surface

$k$  is the wave number ( $k=2\pi/\lambda$ )

$\lambda$  is the wavelength in cm.

The Dubois model was developed for a bare soil or region with very low vegetation with having NDVI <0.4.

The description of all these model and comparison is given in [19]. The use of Dubois model for very low vegetation areas with NDVI less than 0.11 shows better results for C and L band.

For finding of the soil moisture in methods described above, it required field measurements. But for this the field data available should be of same time as that of satellite measurement.

### **3.3. Semi empirical Backscattering models**

Almost all models try to counter the problem of vegetation in the region. Without removing the effect of vegetation none of the theoretical or empirical methods would work. The incorporation of the effect of vegetation makes the task all the more difficult and cumbersome. Many approaches were given by Attema and Ulaby by developing a water cloud model for first order radiative transfer model. This model is chosen because of the simple nature of its application in inversion and also it is able to represent the plant with leaf dimensions smaller than the sensor wavelength. The formulation of the model works even for cases when the size of leaf is smaller than the sensor wavelength.

Because of the size of leafs of canopy being smaller than the wavelength used so the estimation of soil moisture becomes all the way more difficult. So to tackle this problem the vegetation region is estimated as cloud of water droplets held in space by dry structure around. The vegetation is considered a homogenous horizontal cloud with fixed thickness over the soil surface.

The scattering of the radar signal takes place in three ways as shown in figure below. Three types of interaction can take place between the radar signal, soil surface and plant. The signal can be reflected from only plants, or it can be reflected from soil or it could come from multiple reflections between soil and plant. But this multiple reflection is neglected because of the two way attenuation between the soil and plant. The cloud density considered in this model can be estimated to be constant and proportional to the volumetric water content of the

canopy. The height of the canopy is considered an important factor in the development of this model. The values generated are shown below

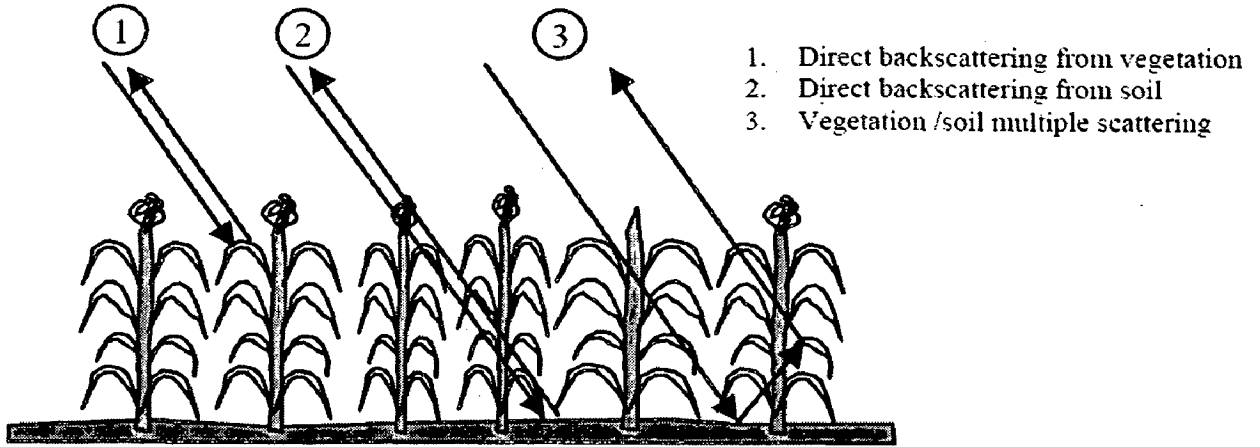


Fig 9: Backscattering of signal from soil as well as vegetation [23]

The total backscatter from a vegetated soil surface is given by three components:

Backscatter from bare soil surface ( $\sigma_{soil}^0$ ),

Direct backscatter of the vegetation layer ( $\sigma_{veg}^0$ )

and multiple backscattering ( $\sigma_{soil+veg}^0$ ) from vegetation and ground surfaces [24, 10]

For the given incidence angle, the total backscatter coefficient is given by:

$$\sigma^0 = \sigma_{veg}^0 + \sigma_{soil+veg}^0 + \tau^2 \sigma_{soil}^0 \quad (3.14)$$

Where  $\tau^2 = e^{(-2B \cdot M_v \cdot Wc)}$

And backscatter from vegetation is given by

$$\sigma_{veg}^0 = A * M_v * \cos\theta (1 - \tau^2) \quad (3.15)$$

Where  $\tau^2$  is the two way attenuation through vegetation.

$M_v$ = volumetric soil moisture content,

$Wc$ = vegetation water content in kg/m<sup>2</sup>

$\theta$  =radar incidence angle.

$A$ = vegetation scattering

And  $B$ = vegetation attenuation

The values of  $A$  and  $B$  are determined from the experimental observations.

This vegetation effect was further studied and implemented by the following factor such as the correlation length. Correlation length can be defined as the distance over which the variation in height of vegetation doesn't change much. The length is an exponential function of a vegetation parameter. This concept is used and included in the water cloud model [14]. The modified expression after including the correlation length came out as follows:

$$\sigma^0 = \sigma_{veg}^{0*} + \tau^2 \sigma_{soil}^0 \quad (3.15)$$

The term  $\sigma_{soil+veg}^0$  being neglected because of the two-way attenuation, this value decreases to very less.

$$\sigma_{veg}^{0*} = \sigma_{veg}^0 (1 - e^{-\alpha}) \quad (3.16)$$

This term represents the value of average distance of the canopy being related to the nearby height of the vegetation. Now this expression gives a relation between the bare soil backscattering coefficients and the vegetation backscattering coefficient. This value of  $\sigma_{soil}^0$  is computed by the regression analysis done using the ground truth values and the theoretical model developed by Dubois. The measured backscatter for different polarizations is the sum of the volumetric soil moisture [7]

### 3.4. Relationship between Moisture and backscattering coefficient

The models described above are little complex in nature as they require not only satellite data but also ground truth data which is not easy to obtain over a vast region. The need for developing a model which could use fewer values of ground truth data and develop a linear relation between the backscattering values and soil moisture is the main area of interest and many researchers gave their respective models. [22-26].

But this moisture is not dependent on one particular soil parameter alone but on many quantities. The many models developed tried to counter these approaches and develop a relation which was suitable for specific land type condition and gave good results under certain constraints. The model developed by [7] gave a simple relation as shown below

$$\sigma_0 = a * M_v + b \quad (3.17)$$

Where  $a$  and  $b$  are empirical coefficients and

$M_v = \text{volumetric soil moisture}$



Backscatter values are in dB

In the early eighties, [26] used a C-band scatterometer that was mounted on a crane to determine the soil moisture in agricultural areas. The experiment was carried out on three different types of soil surfaces for different vegetation. Many experiments of similar nature were carried out for corn, oat and pasture land [49]. Using of different polarization helped in better regression of models for all kind of techniques. The presence of vegetation reduces the visible effects of the soil moisture as the reflection comes directly from the top surface and some from the bottom layer. For burned watershed the values of L band data is higher than the other data. This vegetation factor is an extra factor which has to be accounted for the value generation of data. Various complex and nonlinear methods have been applied to the data available and the output obtained is then measured.

To include the effect of vegetation, various relations are developed to calculate moisture from the vegetated areas. Various relations are developed which include the effects like vegetation water content, vegetation roughness, vegetation temporal SAR backscatter etc. One such relation was developed as shown in equation 3.18: [28]

$$\sigma_0 = a * V_{sm} + b + c * W_{veg} \quad (3.18)$$

Where  $c$  represents the coefficient attenuation by the canopy.

$a$  and  $b$  are found by ground truth measurements

$W_{veg}$  is the vegetation water content

The authors have found that, by using the vegetation corrected factor, the correlation improves significantly (11%) compared to the linear relationship of backscatter and soil moisture.

The ratio of backscatter values of two different days was used as explanatory variable in a simple linear regression model to estimate soil moisture. A normalized soil index is given by in [27] known as Normalized Backscatter Soil Moisture Index (NBMI) reduces the common multiplicative effect of difference in soil type and surface roughness on radar backscatter as it uses backscattering values from two different time intervals.

$$NBMI = \frac{\sigma_{t1} - \sigma_{t2}}{\sigma_{t1} + \sigma_{t2}} \quad (3.19)$$

$\sigma_{t1}$  and  $\sigma_{t2}$  are backscattering coefficients at different time steps

$$V_{sm} = a * \left( \frac{\sigma_{r1}}{\sigma_{r2}} \right) + b \quad (3.20)$$

Here  $V_{sm}$  is the volumetric soil moisture and a and b are empirical parameters that would be can be calculated using the ground truth measurements.

Using the combined effect of NDBI (Normalized Difference Built-up Index and NDVI the effect of vegetation is better encountered to give more accurate soil moisture values [27].

### 3.5. Effect of Vegetation on Soil Moisture Estimation

Effect of vegetation on the moisture estimation of soil is very much taken into consideration. The effect of type of crop, the amount of vegetation, the incidence angle, polarization and frequency are taken into considerations. [7]

These parameters are responsible to make the relationship between SAR backscattering and soil moisture more complex. The vegetation effect on the total backscatter measured by the sensor is mainly due to the macrostructure of vegetation canopy such as height of canopy and number of plants or trees per unit area; and the microstructure, which refers to geometry, moisture contents, and vegetation volume fraction of canopies. The penetration depth radar beam is lower at higher soil moisture contents in vegetation canopies.

The total value of backscatter from the soil depends on vegetation, soil, and the two way reflection which depends on double bounce between the soil and vegetation. The relation between this can be summed up in the following relation as the backscattering effect by vegetation and a loss term dependent on the backscattering term dependent on backscattering value from soil. The vegetation canopy affects the backscattered energy in two ways: first, the vegetation layer attenuates the soil backscatter contribution and second, the vegetation canopy contributes its own backscatter. The total backscattering is composed of backscatter from vegetation and soil, and attenuation / backscatter caused by vegetation ( $\sigma_c$ ) canopy [32]. The relation is shown below in terms of equations (3.21). The total amount of attenuation and backscatter depends on the value of vegetation height, leaf Area Index (LAI). The equation of measured radar backscatter ( $\sigma$ ) from vegetated area has been defined as:

$$\sigma = \sigma_c + f \sigma_b \quad (3.21)$$

The first term is the backscattered value directly from the vegetation. The second value is from the soil which is multiplied by the loss factor  $t$ . The term of vegetation is better realized from the L parameters. The higher the values of L band are used to get the relations. The higher the wavelength the more is the penetration. Not only it depends on vegetation amount but also depends on vegetation moisture content and also vegetation height and correlation length. This two ways travelling in the vegetation leads to losses.

The sensitivity of the interaction of radiation with the overall P and L bands is the guiding factor of soil moisture estimation. The lower wavelengths are more sensitive to soil moistures and the higher wavelengths are sensitive to the more penetration and thus helpful in utilizing of soil moisture values. P and L bands are more sensitive to the vegetation characteristics and thus helpful in moisture detection in vegetation region while the C band values are more related to the bare soil moisture estimation [23]. The microwave signal is attenuated in large quantity by vegetation at higher incidence angle. The horizontal polarizations (HH and HV) have shown higher sensitivity to vegetation and also dependent on the wavelength of the signal. This vegetation effect when combined with the incidence angle effect then it shows great variations. The lower incidence angles show a lower scattering variations and the maximum value is scattered back to the satellite. While the higher value is scattered to the other directions and the effects are not visible. The best configuration is when the incidence angle is close to nadir angle. Further, the microwave signal is less sensitive to leaf area index (LAI) at higher incidence angle.

At a higher incidence angle the rough canopy, due to higher dry matter, which is dominant, generate more scattering than canopy moisture. At higher incidence angle, the radar viewing to the canopy is more through the sides, which reduce the sensitivity to LAI.

The dimension, thickness, and abundance of leave also play an important part in the moisture estimation. The high correlation up to 99% has been found in wheat field having low leaf area index. However, the backscatter from pasture field with large leaf area index cannot be correlated to the soil moisture [29]. For this the first step is to normalize the effect of vegetation and then get the normalized backscattering values. These values are then assumed to have an effect of only the soil moisture and very little or no relation to the vegetation effect.



# Chapter 4

## Study area and the data sets used

---

For this thesis work two types of satellite data are used: PALSAR data and MODIS data.

Both of these data are of the same region. Two sets of satellite images comprising Roorkee city, Manglaur town (Uttarakhand, India) and its surrounding areas were chosen for the study. The satellite images used for the development of algorithm and the validation are ALOS-PALSAR (Advanced Land Observing Satellite – Phased Array type L-band Synthetic Aperture Radar), a SAR data and MODIS (Moderate-resolution Imaging Spectroradiometer), an optical data.

The region is shown in map as below

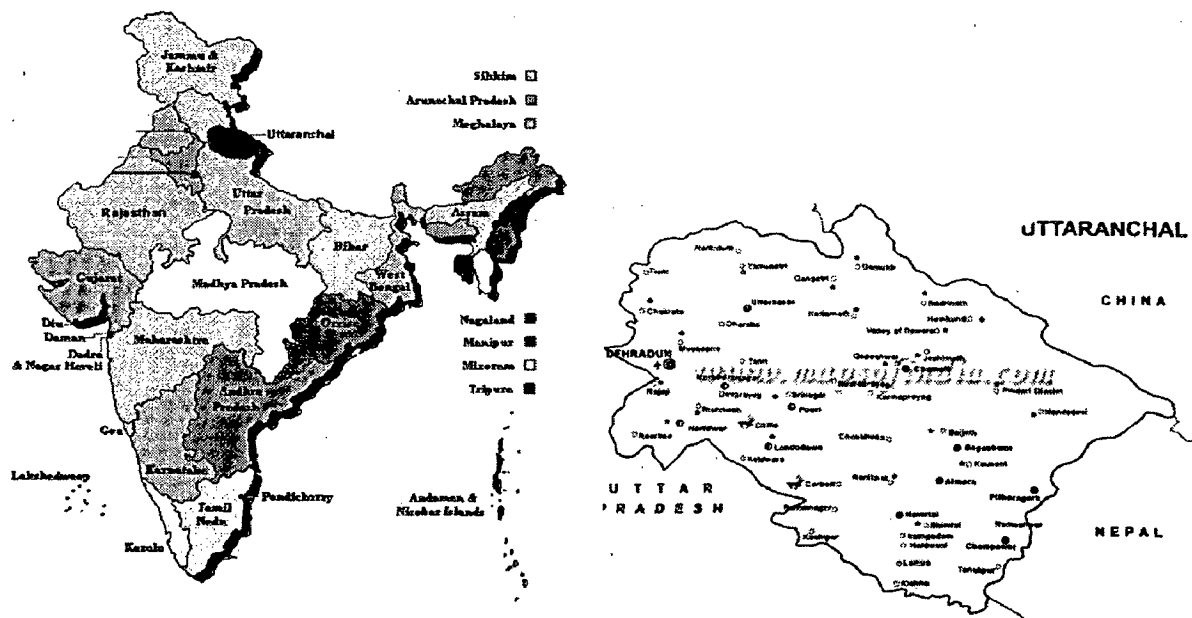


Fig 10: Study region used for this thesis

## 4.1. PALSAR DATA

The Phased Array L-Band Synthetic Aperture Radar (PALSAR) is an active microwave sensor, which is not affected by weather conditions and operates both in daytime and night time. It is improvement based on Synthetic Aperture Radar (SAR) onboard the first earth observation satellite (JERS-1). PALSAR can make observations of the earth regardless of the time of the day, or weather conditions. PALSAR data have many applications, including assessment of ground deformation and forest biomass.

Details of Data used

### PALSAR Data:

Data id: ALPSRP277830590

Date of data: 11/April/2011

### 4.1.1. Preprocessing of PALSAR data

The data available is not in a readable form and hence it has to be preprocessed to further carry out the required analysis of data. The preprocessing is done using the ENVI software.

The main steps in preprocessing of the data are as shown below.

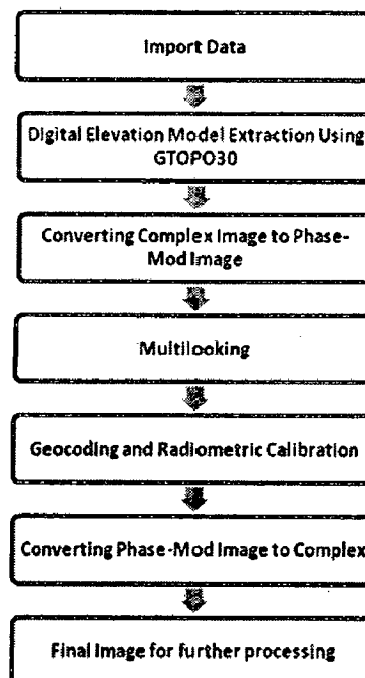


Fig 11: Steps involved in preprocessing of PALSAR data

This image is having complex parameters. To get the value of desired backscattering parameter. The following step is performed

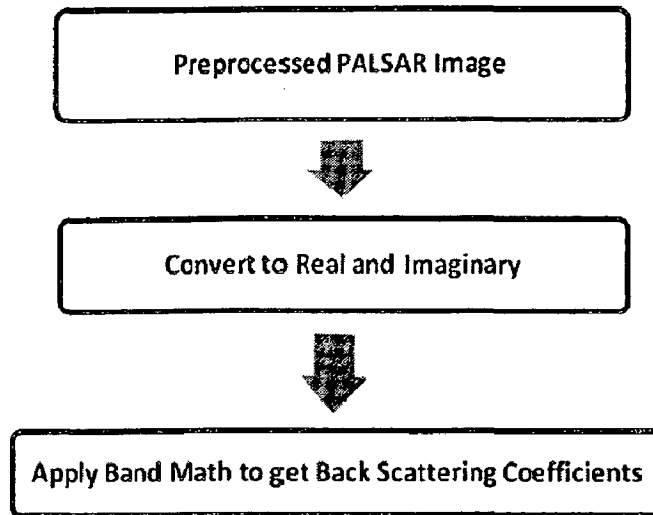


Fig 12: Steps involved in obtaining the backscattering coefficients from PALSAR image

#### 4.2. MODIS DATA

The Moderate-resolution Imaging Spectroradiometer (MODIS) is a payload scientific instrument launched into Earth orbit by NASA. The instruments capture data in 36 spectral bands ranging in wavelength from 0.4  $\mu\text{m}$  to 14.4  $\mu\text{m}$  and at varying spatial resolutions (2 bands at 250 m, 5 bands at 500 m and 29 bands at 1 km).

##### **MODIS data:**

Data id: MOD09Q1.A2011097.h24v06.005.2011109183815

Date of data: 19/April/2011

Preprocessing of MODIS image is already available in the 7bands format which we require.

So not much preprocessing of MODIS image is required.

Directly the different indices required from the image are calculated and then processed.





# Chapter 5

## Methodology

---

### 5.1. Methodology for Land cover classification using satellite data

Classifying land cover into various classes is a very crucial step before any further study is carried out on estimation of soil feature. Classification separate different classes into different regions which can be said to exhibit similar properties. Each region of land cover can be broadly classified into various classes such as Urban, Water, bare soil, moderate vegetation and dense vegetation. Classification of soil into various classes helps in better planning of resources and makes the study of soil characteristics easier. Different land cover classes exhibit different spectral behavior for optical region which can be utilized efficiently to correlate that particular region to a particular class. The advantage lies in the fact is that many frequency bands are available between 620nm to 2155nm with each band showing strong reflectance property with any one feature of a class. Using the variation in reflectance properties for various classes various indices are defined which represent a measure of presence of particular feature of a class. For example Normalized Difference vegetation Index (NDVI) is strongly associated with the density of vegetation. Similarly many other indices are available for vegetation like Enhanced Vegetation Index (EVI), Global Environment Monitoring Index (GEMI), Modified soil adjusted vegetation index (MSAVI), Purified Adjusted Vegetation Index (PAVI) etc. Normalized Difference Building Index (NDBI) is used for estimation of building structures. Similarly Normalized Difference Water Index (NDWI) and Band1 of MODIS are used for detecting presence of water [30, 31, 32, 33, 34, and 35].

The different indices are as follows:

- 1) Normalized Adjusted Vegetation Index (NDVI) [53]

$$NDVI = (\rho_{nir} - \rho_{red}) / (\rho_{nir} + \rho_{red}) \quad (5.1)$$

- 2) Modified Soil Adjusted Vegetation Index (MSAVI) [51]

$$MSAVI = ((2\rho_{nir} + 1) - ((2\rho_{nir} + 1)^2 - 8(\rho_{nir} - \rho_{red}))^{0.5}) / 2 \quad (5.2)$$

3) Purified Adjusted Vegetation Index (PAVI) [55]

$$PAVI = (\rho_{nir}^2 - \rho_{red}^2) / (\rho_{nir}^2 + \rho_{red}^2) \quad (5.3)$$

4) Global Environment Monitoring Index (GEMI) [52]

$$GEMI = \xi(1 - 0.25\xi) - (\rho_{red} - 0.125) / (1 - \rho_{red}), \quad (5.4)$$

$$\xi = (2(\rho_{nir}^2 - \rho_{red}^2) + 1.5\rho_{nir} + 0.5\rho_{red}) / (\rho_{nir} + \rho_{red} + 0.5)$$

5) Enhanced vegetation index [53]

$$EVI = 2.5 \frac{(\rho_{nir} - \rho_{red})}{(L + \rho_{nir} + C_1\rho_{red} + C_2\rho_{blue})} \quad (5.5)$$

All these indices are used to classify the vegetation and bare soil region of a land

Apart from these indices the following two indices are also available.

6) Normalized difference built up index[54]

$$NDBI = (band5 - band4) / (band4 + band5) \quad (5.6)$$

The values calculated by the first five equations are directly correlated to the vegetation index of the soil the vegetation. The higher is the value of these indices the higher is the value of vegetation. The values lie between -1 to +1. With values less the 0 representing either water region or urban region. But the water and urban region respond to the positive values also.

Steps followed for classification of image using different indices is as follows:

**Step 1:** Calculate the value of indices value for all images and try to calculate the separate one class from the other. The class having the highest separability from other classes is classified into one class and the rest are classified as remaining classes.

**Step 2:** For this class calculate the vegetation indices EVI, NDVI, GEMI, MSAVI, and PAVI and also calculate NDBI and NDWI.

- Step 3: For that particular classified class try to get the threshold values of different indices for that particular land cover class.
- Step 4: So in this way the first class is classified. Now do the same step to the remaining classes. Find out the values of indices for the remaining classes.
- Step 5: For the remaining classes check out the best possible second class which exhibits the best contrasting reflectance values with respect of the remaining classes.
- Step 6: Repeat the procedure again and classify the remaining classes using all the indices.

The flowchart of the whole process is shown in the figure shown below

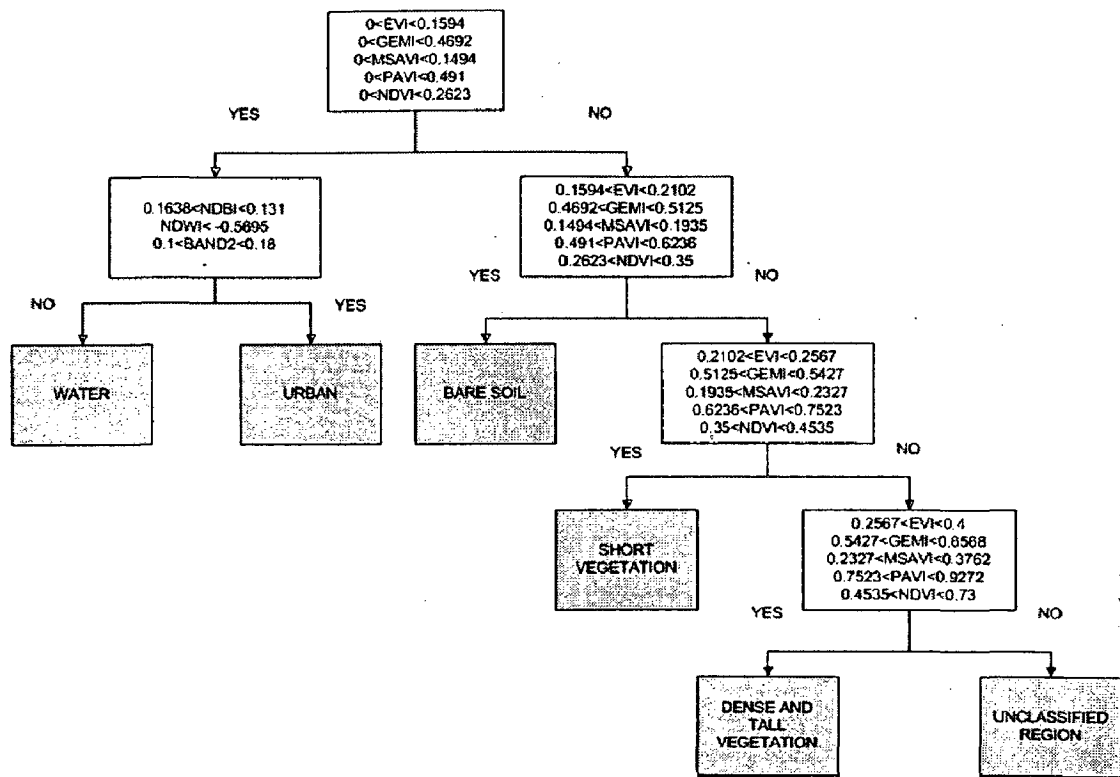


Fig 13: Finally applied decision tree on the MODIS image

## 5.2. Methodology for soil moisture estimation using satellite data

First step in calculating the soil moisture is the normalization with respect to vegetation effect. After normalizing the vegetation effect the next step is applying the inversion approach for moisture retrieval.

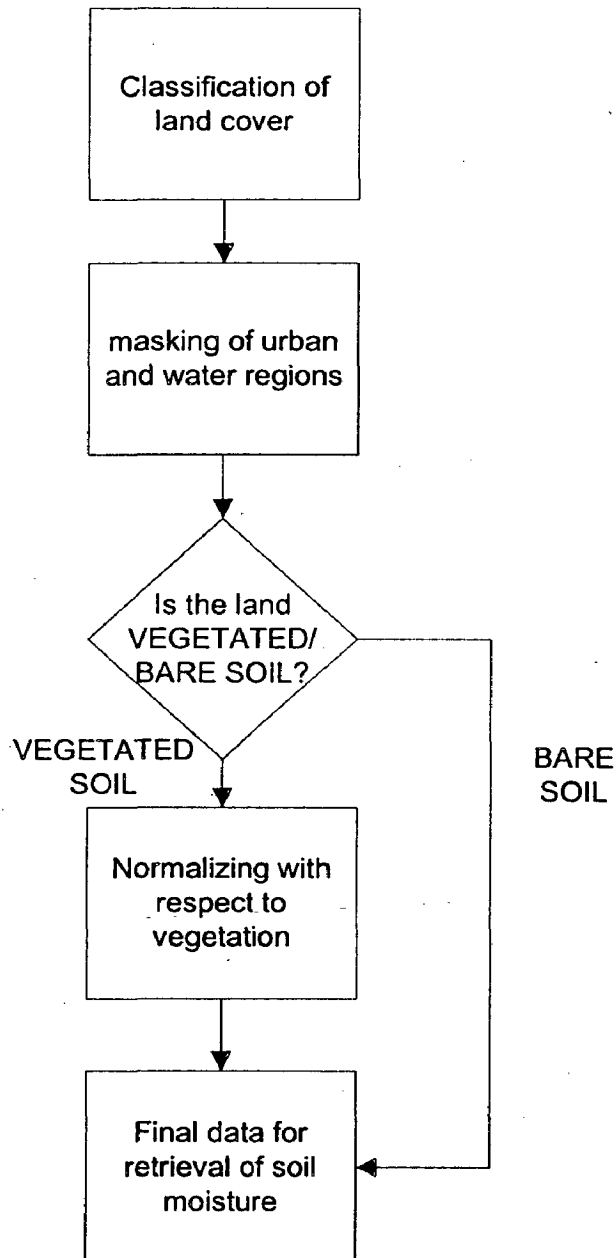


Fig 14: Initial normalization of data with respect to vegetation

### **5.2.1. Steps to obtain SAR data normalized with respect to vegetation**

The overall steps of retrieval of soil moisture as depicted in the flowchart above are explained in detail above:

Various steps in overall methodology are explained below:

#### **Step 1. Preprocessing of SAR**

SAR data is preprocessed as mentioned in section 4.1.1

#### **Step 2. Classification MODIS image into various land cover classes**

MODIS image is classified into different land cover classes as mentioned in section 5.1

#### **Step 3. Masking of water bodies and urban area of PALSAR image**

The moisture values of urban areas and water bodies have no physical significance as our main objective is to extract moisture from soil.

The overall masking is done in following three steps

- The spatial resolution of PALSAR and MODIS image is 25 m and 250 m, respectively. Therefore, the averaging of  $10 \times 10$  pixel of PALSAR image has been performed to match the resolution of PALSAR image with MODIS image.
- The rescaled PALSAR image was co-registered with classified MODIS image.
- After co-registration of PALSAR image the region is of urban and water regions are masked

#### **Step 4. Normalizing the effect of vegetation**

After masking the urban and water regions, the area remaining are the bare soil and vegetated areas. The moisture value of vegetated area is directly computed from different inversion approaches mentioned in next section but the vegetation effect creates a problem as they interfere with the radar backscattered signal and thus introduce biases in soil moisture retrieval results. Therefore the effect of vegetation has to be normalized to get correct backscattered values which are then preprocessed to get soil moisture values. The information content of the image and the vegetation characterization is fulfilled with the utilization of the optical data. The NDVI values from MODIS image are used for vegetation parameter modeling. NDVI values are related to the vegetation parameters and thus NDVI values can be used as a normalizing factor to normalize the SAR backscattered values.

This overall normalization of vegetation cover is explained below:

The scattering coefficient is dependent on sensor parameters as well as surface parameters. As the sensor parameters are known, only the surface parameters are to be studied and normalized with respect to vegetation.

The scattering coefficient obtained from satellite data is dependent on overall surface factors which are a summation of vegetation, soil concentration (di-electric constant) and surface roughness [43].

Overall the relation can be represented as follows

$$\sigma_{PP\ Image}^0 = f(\text{Vegetation , dielectric constant of moist soil, surface roughness}) \quad (5.8)$$

Where  $\sigma_{PP\ Image}^0$  = backscattering coefficient obtained from satellite image

PP in the subscript is used for HH and VV data.

Excluding the effect of vegetation the di-electric constant and surface roughness can be attributed as one quantity the soil parameters.

The relation can be rewritten as

$$\sigma_{PP\ Image}^0 = f(\text{Vegetation , Soil parameters}) \quad (5.9)$$

The scattering coefficient of bare soil (i.e.,  $\sigma_{PP\ Soil}^0$ ) depends on soil parameters, i.e. dielectric constant and surface roughness is represented as given by equation

$$\sigma_{PP\ Soil}^0 = f(\text{Soil parameters}) \quad (5.10)$$

From equations it can be seen that the normalizing  $\sigma_{PP\ Image}^0$  with respect to  $\sigma_{PP\ Soil}^0$  a normalized coefficient which is only as a function of vegetation characteristics. The different images available for the same area of interest are with the different polarization (HH-, HV-, VH- and VV-polarization). So that, in the case of PALSAR image, with the availability of different polarization images, the normalized scattering coefficient ( $\Delta\sigma_{PP}^0$ ) can be written as Equation 6.4, where PP represent for HH-, VV- or HV-polarization. [43]

$$\Delta\sigma_{PP}^0 = \frac{\sigma_{PP\ Image}^0 (\text{Vegetation , Soil parameters})}{\sigma_{PP\ Soil}^0 (\text{Soil parameters})} = f(\text{Vegetation}) \quad (5.11)$$

$\Delta\sigma_{PP}^0$  can be correlated with other vegetation parameter like NDVI, which represent the vegetation function only. So, there is a need to develop relationship between  $\Delta\sigma_{PP}^0$  and NDVI for characterization of  $\Delta\sigma_{PP}^0$ . In the present case for the development of the soil moisture retrieval in vegetation covered area, HH- and VV-polarization have been taken into account. Therefore, PP will represent either HH- or VV-polarization only. [43]

The aim for calculating of  $\sigma_{HH\ Soil}^0$  and  $\sigma_{VV\ Soil}^0$  by is building a forward model which depends on ground truth values and backscattered values obtained from image. The ground truth values are calculated for 30 test areas were chosen for in situ measurement of soil moisture and surface roughness under the vegetation cover at the time of image acquisition. With the ground truth values the backscattering values were calculated by using the Dubois model [23].] In HH-polarization ( $\sigma_{HH\ Soil}^0$ ) and VV-polarization ( $\sigma_{VV\ Soil}^0$ ). Dubois *et al.* [23] model has been utilized as it provides the direct relationship between the scattering coefficient in HH- and VV-polarization and soil parameters (i.e., soil moisture and surface). Further, Dubois *et al.* [23] model can be solved to provide the dielectric constant of soil as function of scattering coefficient in HH- and VV-polarization and does not require the characterization of soil surface roughness [23]

$$\sigma_{HH\ Soil}^0 = 10^{-2.75} \frac{\cos^{1.5} \theta}{\sin \theta^5} 10^{0.028\epsilon \tan \theta} (ks \sin^{1.4} \theta) \lambda^{0.7} \quad (5.12)$$

$$\sigma_{VV\ Soil}^0 = 10^{-2.35} \frac{\cos^3 \theta}{\sin \theta} 10^{0.046\epsilon \tan \theta} (ks \sin^3 \theta)^{1.1} \lambda^{0.7} \quad (5.13)$$

The required input parameters in Dubois equations are rms surface height (s) and dielectric constant ( $\epsilon$ ) as soil parameters and incidence angle ( $\theta$ ) and wavelength ( $\lambda$ ) as sensor parameters. Incidence angle and wavelength are 24° and 23.6 cm, respectively for PALSAR image of the study area. The dielectric constant ( $\epsilon$ ) of soil can be measured with the empirical relationship provided by Equation

$$\varepsilon = 3.03 + 9.3m_v + 146m_v^2 - 76.7m_v^3 \quad (5.14)$$

here  $m_v$  is the volumetric soil moisture content

The characterization of surface roughness in form of rms surface height ( $s$ ) was also done during the field visit with the help of pin profilometer [55]. The roughness of the field during the observation was found to be approximately constant and the average rms surface height was observed 0.53 cm with standard deviation 0.06 cm.

The Normalized Difference Vegetation Index (NDVI) is almost linearly related to the vegetation abundance and therefore, can represent the vegetation effect in the soil moisture retrieval studies [45]. NDVI is defined as the ratio of the difference and sum of the spectral response at the infrared wavelength (band 2 for MODIS) and red wavelength (band 1 for MODIS) which is written as Equation 6.8.

$$NDVI = \frac{\rho_{NIR} - \rho_{RED}}{\rho_{NIR} + \rho_{RED}} = \frac{\text{Band 2} - \text{Band 1}}{\text{Band 2} + \text{Band 1}} \quad (5.15)$$

Where  $\rho_{NIR}$  and  $\rho_{RED}$  are the reflectance at NIR band and RED band respectively.

As the NDVI value was correlated to the abundance of vegetation. The value of NDVI was used for normalizing the vegetation effect. The higher the value of NDVI is related to the higher the abundance of vegetation.

The relation between  $\Delta\sigma_{pp}^0$  and Normalized difference vegetation index ( $NDVI$ ) is used to normalize the effect of vegetation. The normalized scattering coefficient ( $\Delta\sigma_{pp}^0$ ) is a function of vegetation parameters as well as soil parameters and this is obtained from PALSAR image whereas NDVI which characterizes the vegetation in optical data can be retrieved with MODIS data.

The developed empirical relationship  $\Delta\sigma_{pp}^0$  (dB) is a function of NDVI and is given as Equation

$$\Delta\sigma_{pp}^0 \text{ (dB)} = P_1 \times (NDVI)^2 + P_2 \times (NDVI) + P_3 \quad (5.16)$$



After obtaining the values of  $P_1, P_2, P_3$  and  $P_4$  the function  $f(\text{Vegetation})$  is defined and thus developing a relation between  $\sigma_{\text{PP Image}}^0$  and  $\sigma_{\text{PP Soil}}^0$

$$\sigma_{\text{PP Soil}}^0 (\text{Soil parameters}) = \frac{\sigma_{\text{PP Image}}^0 (\text{Vegetation, Soil parameters})}{f(\text{Vegetation})} \quad (5.17)$$

From this relation the backscattered coefficient values normalized with respect to vegetation effect of the soil are obtained.

### 5.2.2. Retrieval of soil moisture using various inversion approaches

After the SAR data is normalized with respect to vegetation it is normalized with respect to the vegetation the data is used by three different inversion approaches to find out the soil moisture. The three different inversion approaches are used to find stable regions which low variability of soil moisture regions which are then classified into one class. The overall methodology is shown below:

#### 5.2.2.1. Neural Network approach

The advantage of NN technique is that all surface parameters included and trained in neural network acts as an empirical mapping relation between radar backscatter and land surface parameters. In neural network, the system is trained to generate direct relation to between the complex networks of input parameters with that of output parameters. [41, 42]

First the neural network is runs for a testing phase. After the desired response is obtained that then the neural network is tested on the new field.

The overall neural network implemented had the structure as shown in fig: 14

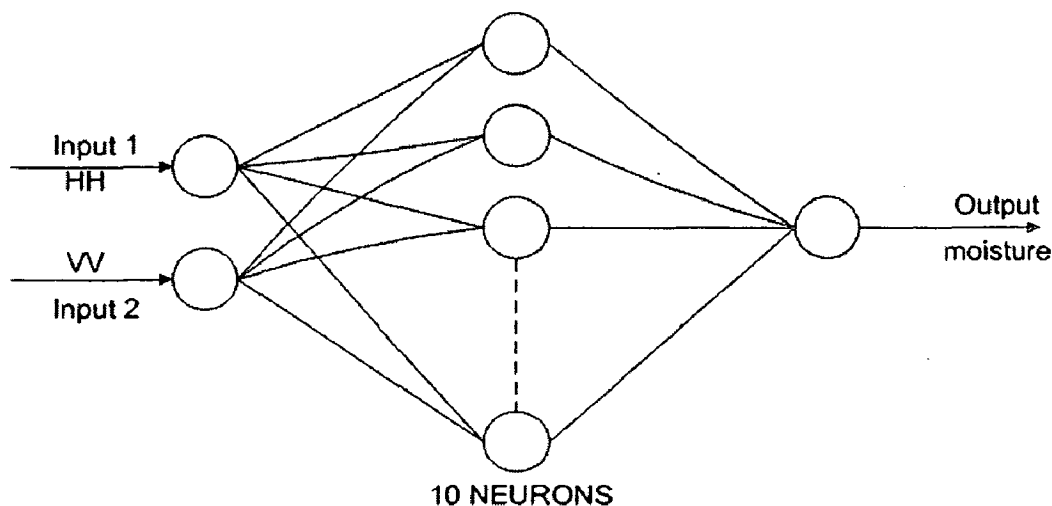


Fig 15: Neural network has an advantage that is adaptive in nature.

Parameters of neural network were as follows:

Number of input neurons	2 (HH and VV values obtained from SAR data)
Number of hidden layers	1 (using one layer gives better results than using more number of layers)
Number of neurons in hidden layer	10 (this program was tested for different neurons and the results obtained were best suited for a 10 layer hidden neurons)
Number of outputs	1 (moisture value)

Table 3: parameters used for designing neural network

### 5.2.2.2. Dubois model for soil moisture estimation

The retrieved scattering coefficient values of the bare soil will contain the information of the soil moisture as well as surface roughness. Dubois equations in HH- and VV-polarization have been solved to provide an equation that is the function of dielectric constant only and independent to surface roughness.

The overall methodology is explained in this flowchart

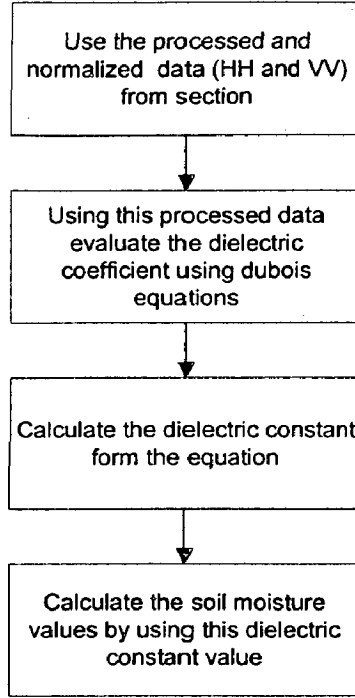


Fig 16: Flow chart for Dubois Model

### Methodology for Dubois model for soil moisture estimation

- i. First the preprocessing of the SAR data is done as explained till the step: 3 above.
- ii. Using this preprocessed data of HH and VV the dielectric constant is calculated as given by the Dubois method

$$\varepsilon = \frac{10 \times \sigma_{VVS_{oil}}^0 (dB) - 11 \times \sigma_{HHS_{oil}}^0 (dB) + 110 \times \log(C_1) - 100 \times \log(C_2)}{1.52 \times \tan(\theta)} \quad (5.18)$$

Where

$$C_1 = 10^{-2.75} \frac{\cos^{1.5} \theta}{\sin \theta^5} (k \sin^{1.4} \theta) \lambda^{0.7} \quad (5.19)$$

And

$$C_2 = 10^{-2.35} \frac{\cos^3 \theta}{\sin \theta} (k \sin^3 \theta)^{1.1} \lambda^{0.7} \quad (5.20)$$

- iii. Using this dielectric constant the soil moisture is directly calculated using the following equation

$$m_v = -5.3 \times 10^{-2} + 2.92 \times 10^{-2} \varepsilon - 5.5 \times 10^{-4} \varepsilon^2 + 4.3 \times 10^{-6} \varepsilon^3 \quad (5.21)$$

Where  $\varepsilon$  is the dielectric constant of soil and  $m_v$

### 5.2.2.3. Nelder-Mead minimization method

This is a direct-search method which works moderately on stochastic problems and commonly used in nonlinear regression problems. In our problem of finding the soil moisture the approach used is to find out the dielectric constant by minimizing the difference between the measured dielectric constant ( $\sigma_{meas}^0$ ) and simulated ( $\sigma_{theo}^0$ ) backscattering data. The theoretical values are obtained using the Dubois model and the measured values are obtained from the satellite data. The model developed is explained below.

The overall model flowchart is explained below:

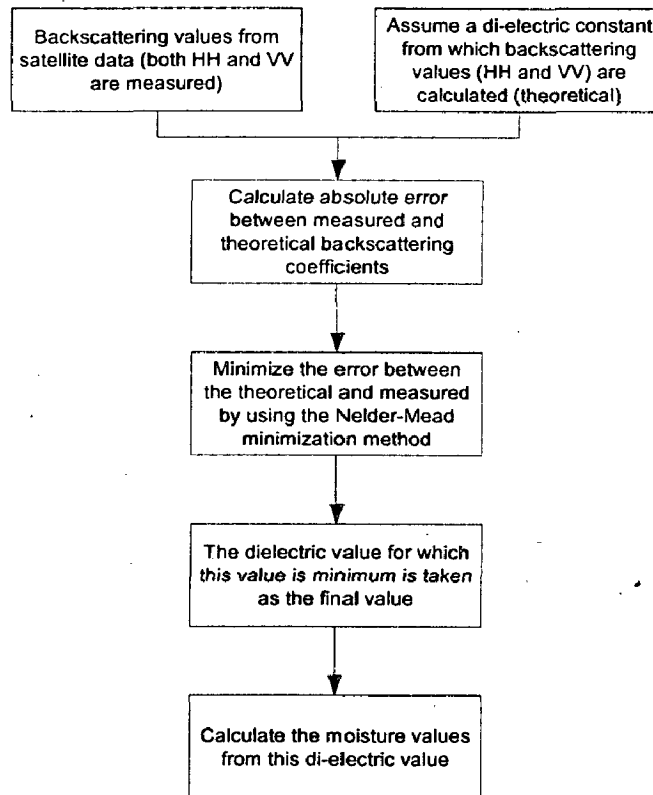


Fig 17: Outline of Nelder-Mead minimization method

### Methodology for Nelder-Mead Approximation

- i. Obtain backscattering values from satellite data.

- ii. Assume an approximate di-electric constant value from which the backscattering values are calculated by Dubois model.
- iii. Calculate absolute error value from this model and try to minimize this using Nelder-Mead minimization function. The variable which is changed to minimize the function is the di-electric constant. The overall aim is to calculate that value of di-electric constant from which the absolute error between the function is minimized.
- iv. The corresponding value from which the absolute error comes out to be minimum is taken as the final value of di-electric constant and this value is



# Chapter 6

## Results and discussion

---

### 6.1. Classification of image

The MODIS data of 36bands and 500mts resolution was used. The main bands which are useful are 1-7bands. The data used of four months spanning from March to May was used. Data used was of the following date's 17/March/2011, 11/April/2011, 19/May/2012, 16/June/2011. The reason behind selected four moths is to compare the variation of crop growth with months.

As seen from the classification table that all the indices are calculated of for the entire image and then the intersection of the common region is taken to get the best possible approximation of the required image. The following were the results obtained by classifying the image using different indices and then taken the intersection of all.

The values that were received for different indices are summarized in the table below:

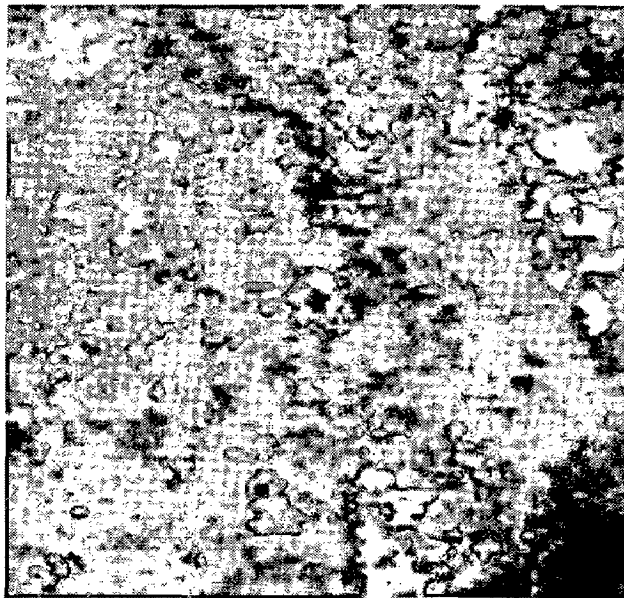


Fig 18: Raw MODIS Image

RANGES OF INDICES			
EVI	urban	0	0.159436
	bare soil	0.159436	0.210184
	short veg	0.210184	0.256736
	tall veg	0.256736	0.400167
GEMI	urban	0	0.4692
	bare soil	0.4692	0.5125
	short veg	0.5125	0.5427
	tall veg	0.5427	0.656818
MSAVI	urban	0	0.149354
	bare soil	0.149354	0.193491
	short veg	0.193491	0.232731
	tall veg	0.232731	0.376163
PAVI	urban	0	0.491
	bare soil	0.491	0.623562
	short veg	0.623562	0.752286
	tall veg	0.752286	0.927196
NDVI	urban	0	0.2623
	bare soil	0.2623	0.35
	short veg	0.35	0.4535
	tall veg	0.4535	0.73

Table 4: Final threshold values obtained for different vegetation contents

The ranges of values for different indices for classifying land into different land cover regions is obtained by calculating the separability index for each pair of class with remaining classes.

After calculating the separability index for those classes the corresponding values for separability classes is taken as the decisive value for classification.

The separability index for the two separating classes is calculated as follows [44]:

$$SI = \frac{|\mu_1 - \mu_2|}{\sigma_1 + \sigma_2} \quad (6.1)$$

Where SI= separability index



$\mu_1$ =mean of class 1

$\mu_2$ =mean of class 2

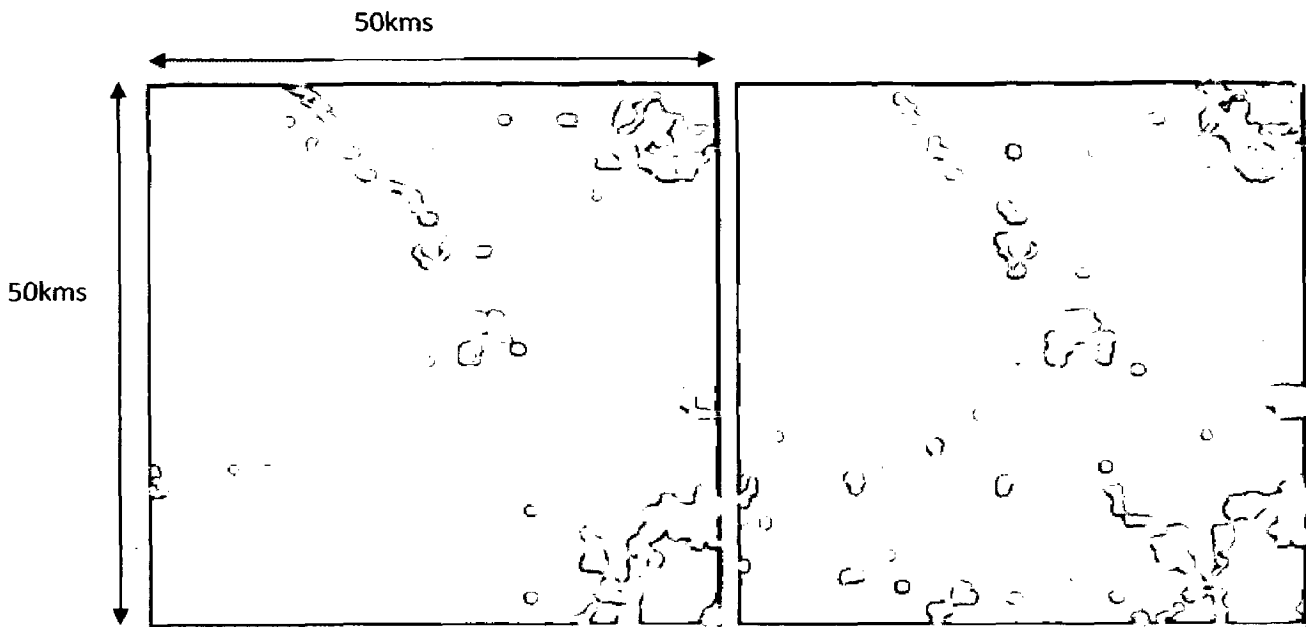
$\sigma_1$ =standard deviation of class 1

$\sigma_2$ = standard deviation of class 2

INDEX	CLASS 1	CLASS 2	SEPARABILITY INDEX
EVI	water	urban, bare soil, short veg, tall veg combined	1.6
	urban	bare soil, short veg, tall veg combined	1.51
	bare soil	short veg, tall veg combined	1.42
	short veg	tall veg	1.4
GEMI	water	urban, bare soil, short veg, tall veg combined	1.633
	urban	bare soil, short veg, tall veg combined	1.56
	bare soil	short veg, tall veg combined	1.43
	short veg	tall veg	1.38
MSAVI	water	urban, bare soil, short veg, tall veg combined	1.6
	urban	bare soil, short veg, tall veg combined	1.49
	bare soil	short veg, tall veg combined	1.43
	short veg	tall veg	1.41
PAVI	water	urban, bare soil, short veg, tall veg combined	1.63
	urban	bare soil, short veg, tall veg combined	1.58
	bare soil	short veg, tall veg combined	1.49
	short veg	tall veg	1.42
NDVI	water	urban, bare soil, short veg, tall veg combined	1.61
	urban	bare soil, short veg, tall veg combined	1.51
	bare soil	short veg, tall veg combined	1.48
	short veg	tall veg	1.41

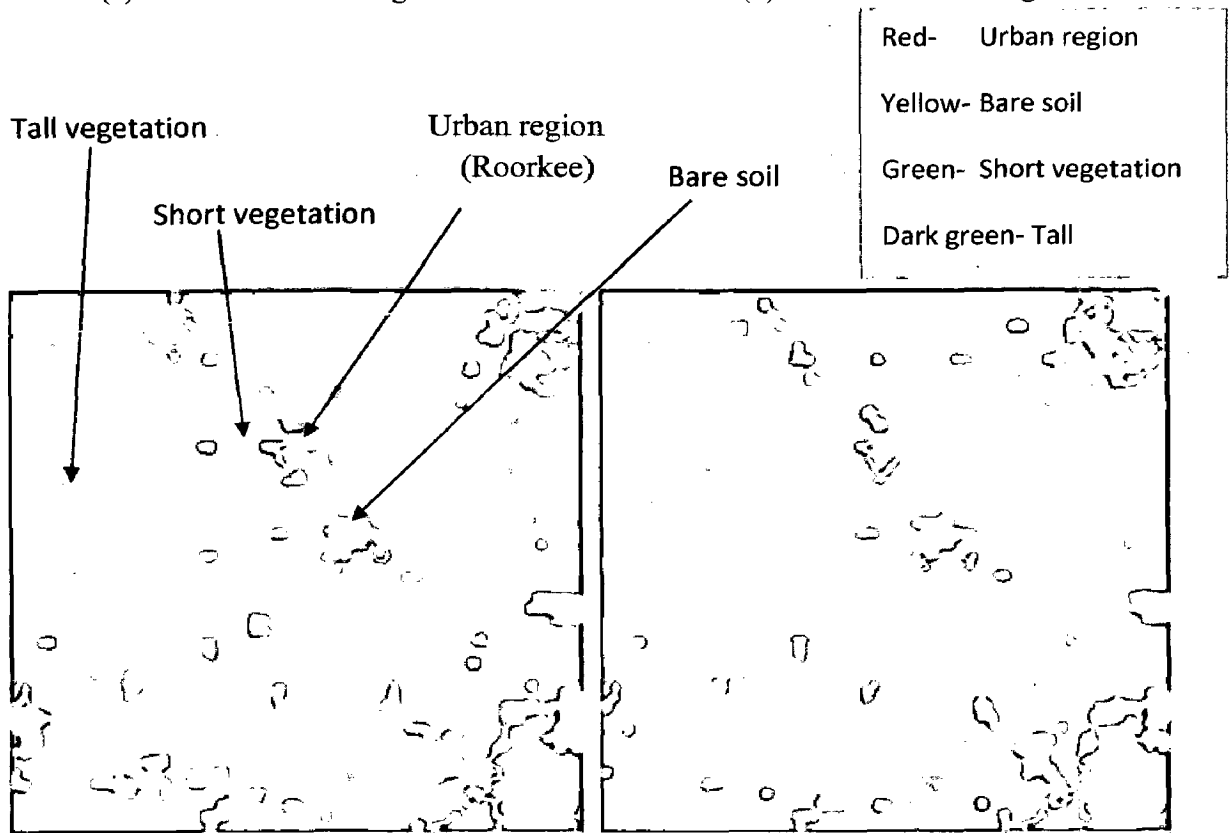
Table 5: Separability index obtained for different land cover classes

The overall steps of classification are mentioned in section 5.1.



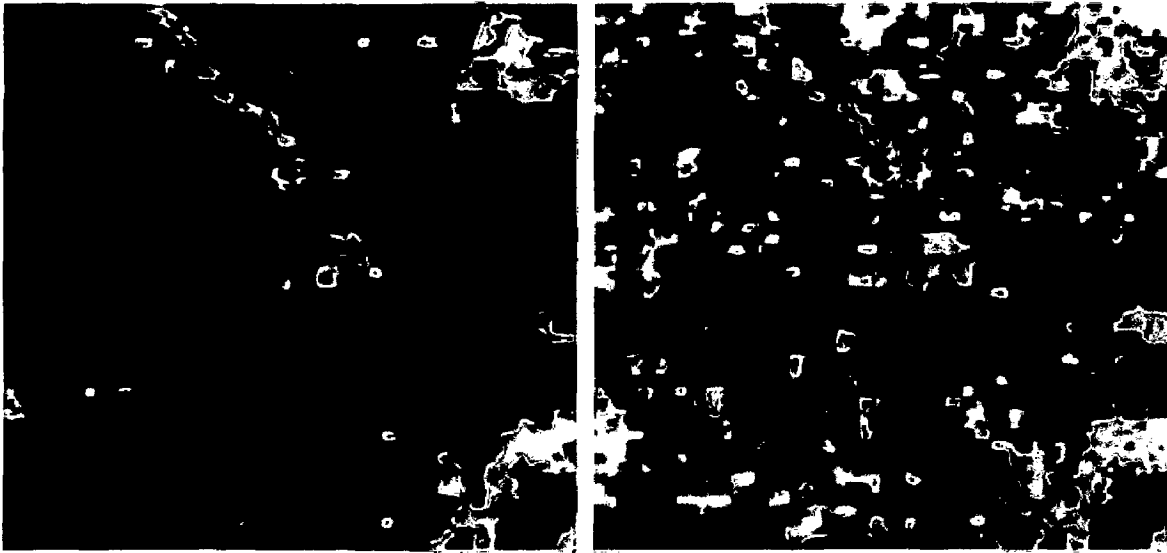
(a) Classification using NDVI

(b) classification using EVI



(c) Classification using GEMI

(d) Classification using MSAVI



(e) Classification using PAVI

(f) Final classified image with common region

Fig 19: Image classified into different regions using various indices.

Red-	Urban region
Yellow-	Bare soil
Green-	Short vegetation
Dark green-	Tall

The above image was for April-2012

The value of accuracy obtained for final image Fig18: (f) obtained by common region of all the classified images from different indices is as follows:

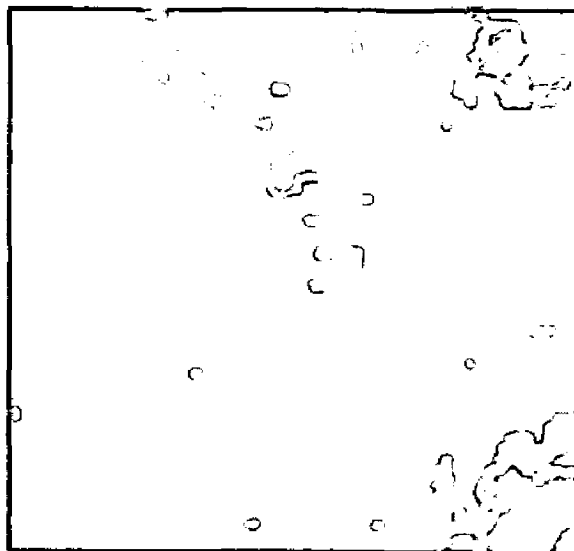
**The Overall Accuracy = 85.1351%**

**Kappa Coefficient = 0.7922**

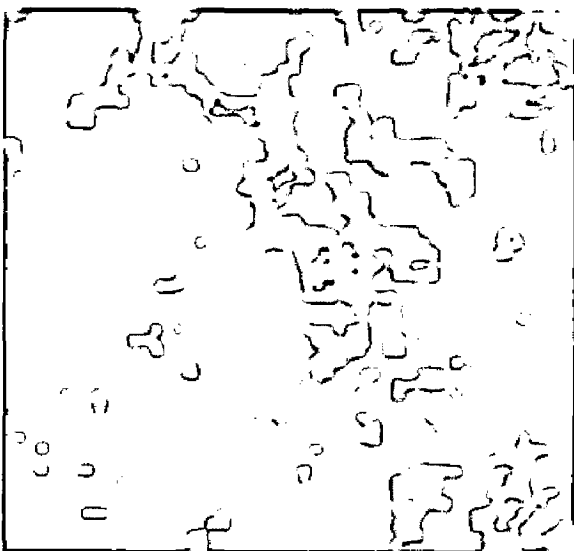
**Comparison between the growths of vegetation for four months**



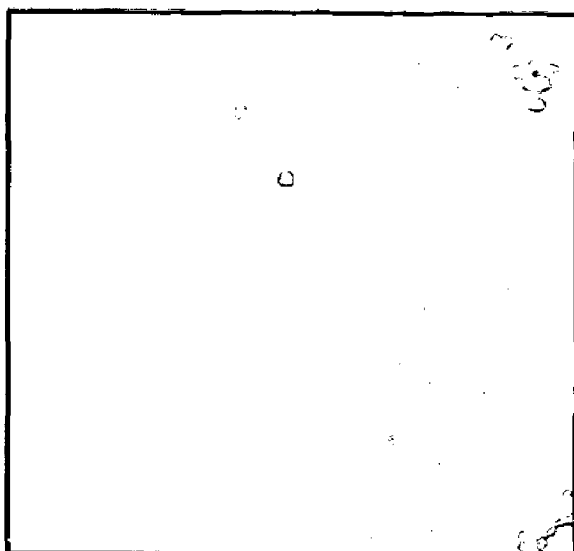
(a) 17-March-2012



(b) 19-April-2012



(c) 19-May-2012



(d) 16-June-2012

**Fig 20: Comparison of growth for four months of (a) March, (b) April, (c) May, (d) June**

## 6.2. Vegetation correction

The overall methodology of vegetation correction is explained in step.4 of section 5.2.1. The flowchart of overall methodology is given below in fig 21.

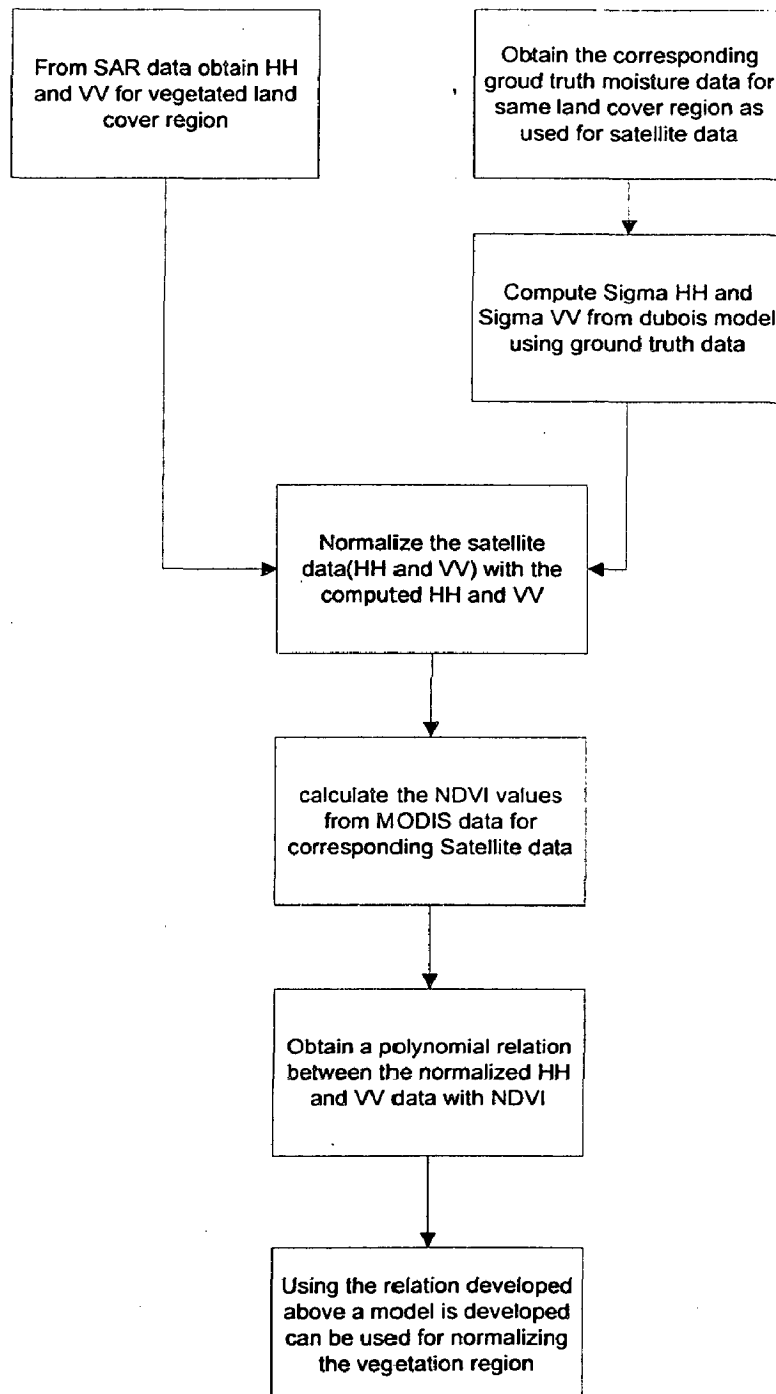


Fig 21: overall outline for vegetation correction

## Steps for vegetation correction

- Step 1: From SAR data obtain the backscattered sigma-HH and sigma-VV values for vegetation land cover region
- Step 2: For same region obtain the corresponding ground truth moisture data. From this moisture data obtain the sigma HH and sigma VV values using the help of Dubois equations compute the dielectric constant using the equation (5.14)
- Step 3: Using the calculated dielectric constant from step 3, now compute the value of sigma HH and sigma VV
- Step 4: As this is the sigma HH and sigma VV are calculated from the soil moisture, these values of HH and VV can be assumed to depend only on soil moisture and does not include any vegetation effect.
- Step 5: Now two data sets are available, one from satellite and one from field visit. Normalize these two data's by dividing the satellite data by calculated data
- Step 6: For the same region calculate NDVI values using the MODIS data.
- Step 7: Resize the SAR data to match with the resolution of MODIS data, which in this case comes out to be factor of 10. So reduce the resolution of SAR by a factor of 10.
- Step 8: For the two data's available in steps 5 and 6. Find a polynomial relation of degree two
- Step 9: The obtained constant values from this polynomial relation are finally used for normalizing the satellite data available for HH and VV.
- Step 10: The results of this normalizing factor are shown in fig 22 and fig 23.

**Final relation between the NDVI values and normalized Sigma-HH and Sigma-VV**

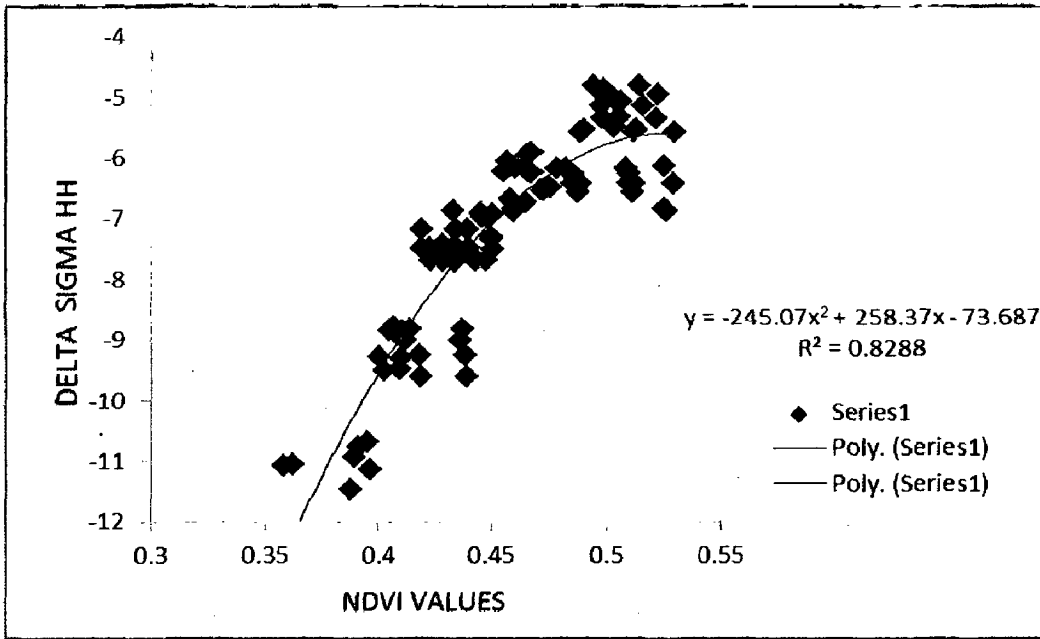


Fig 22 relation between normalized HH with NDVI

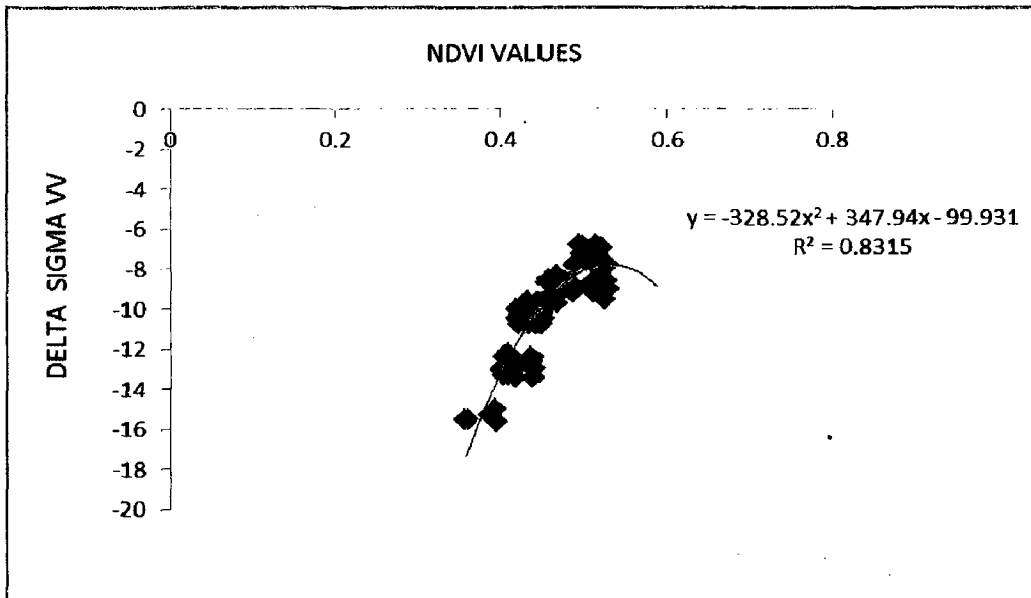


Fig 23 relation between normalized VV with NDVI

### 6.3. Neural Network Approach

Two inversion approaches were applied and the moisture map was generated using the same. The whole process flow is shown in fig 21:

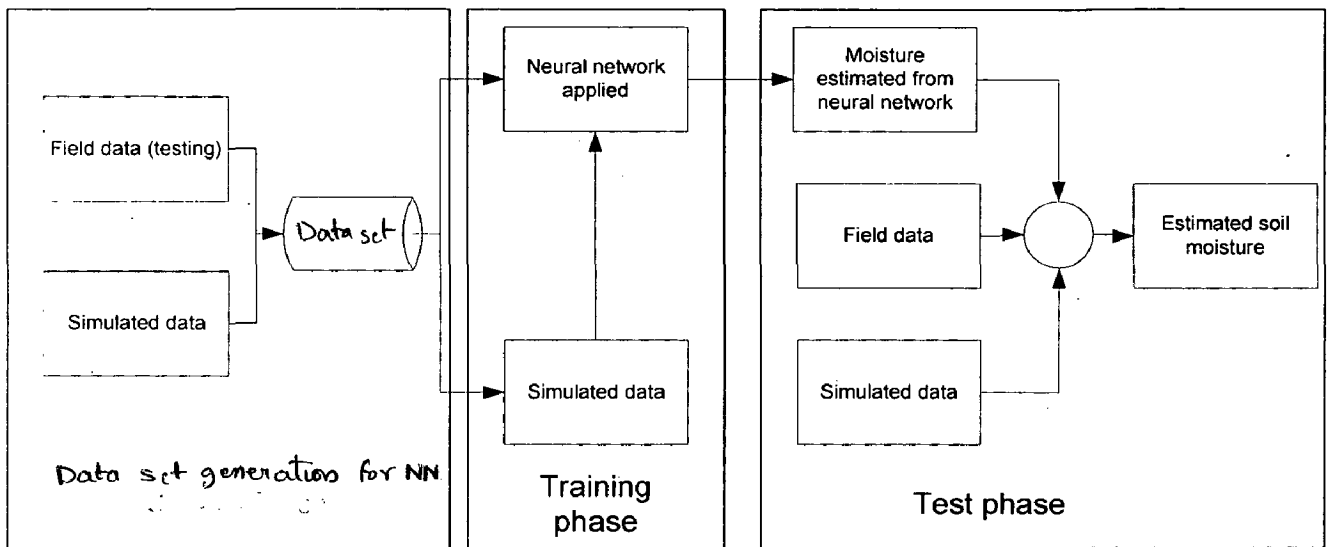


Fig 24: Whole process outflow for development of model for moisture calculation.

Step 1. First the regions were separated for bare soil and vegetated land cover region.

Step 2. Using the field data the forward model for neural network which is known as the training phase is developed for Neural network.

Step 3. In training phase of neural network the model was developed and tested for different number of neurons in hidden layers. The optimum result came out for one hidden layer with having ten neurons.

Step 4. Using this model developed in training phase this model was testing on a different region having testing data generated from the measured data set.

Step 5. The results obtained were tested for measured as well as calculated data set.



One important aspect that was taken into account that the input is backscattering coefficient dB was normalized in the scale of 0 to 1 because neural network optimized for this value quickly and the error was minimal in this case.

The output of neural network was moisture values.

The following figures of merits were calculated:

Mean squared error (MSE)

$$MSE = \frac{1}{k} \sum_{i=1}^k (m_i^m - m_i^p)^2$$

Mean absolute error (MAD)

$$MAD = \frac{1}{k} \sum_{i=1}^k |(m_i^m - m_i^p)|$$

Here the

$m_i^m =$  *measured moisture value*

$m_i^p =$  *predicted moisture value*

Characteristics of neural network during the training and testing phase:

**Result for Training phase:**

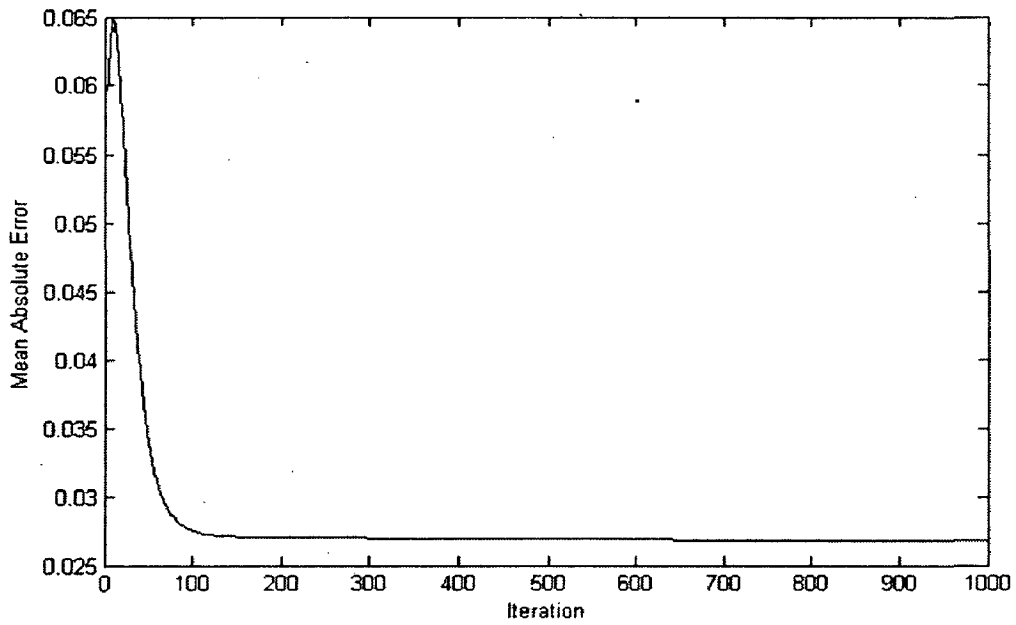


Fig: 25 comparison of mean absolute error with iterations for computing the soil moisture for bare soil

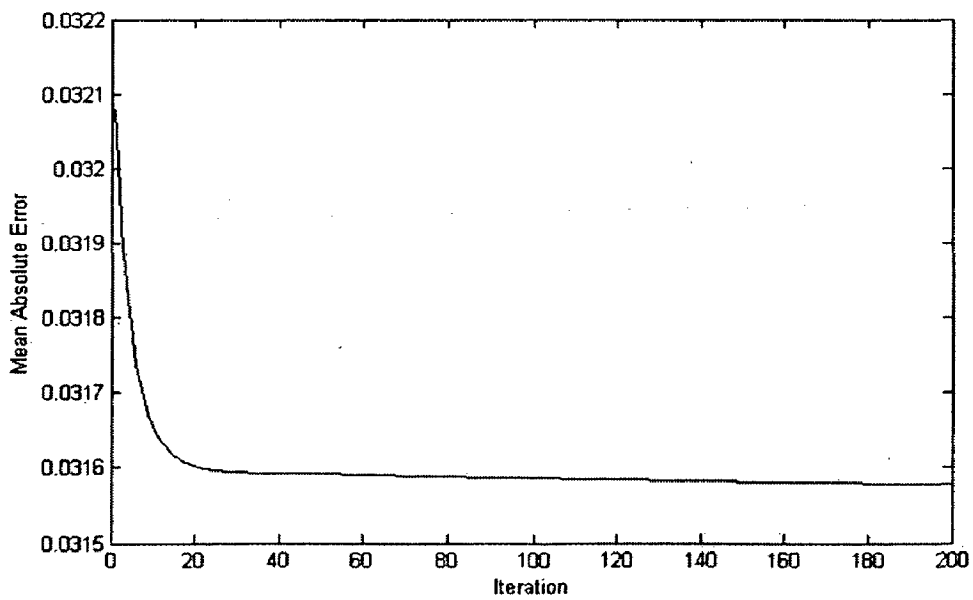


Fig 26: Iterations for training the data in vegetation region.

Neural Network used was three layers, i.e. input, hidden and output layer. The numbers of neurons are two, ten, and one respectively. The number of hidden neurons was optimized on trial basis for better training accuracy. Adaptive learning mechanism was adopted with a factor of 10% reduction in learning rate when network stucked in local minima. Back propagation feed forward algorithm with sigmoid activation function has been used to construct the predictive model. The input and output data points were scaled according to the characteristic of sigmoid function. A small amount of (0.3) momentum factor has been incorporated to avoid oscillations during training phase.

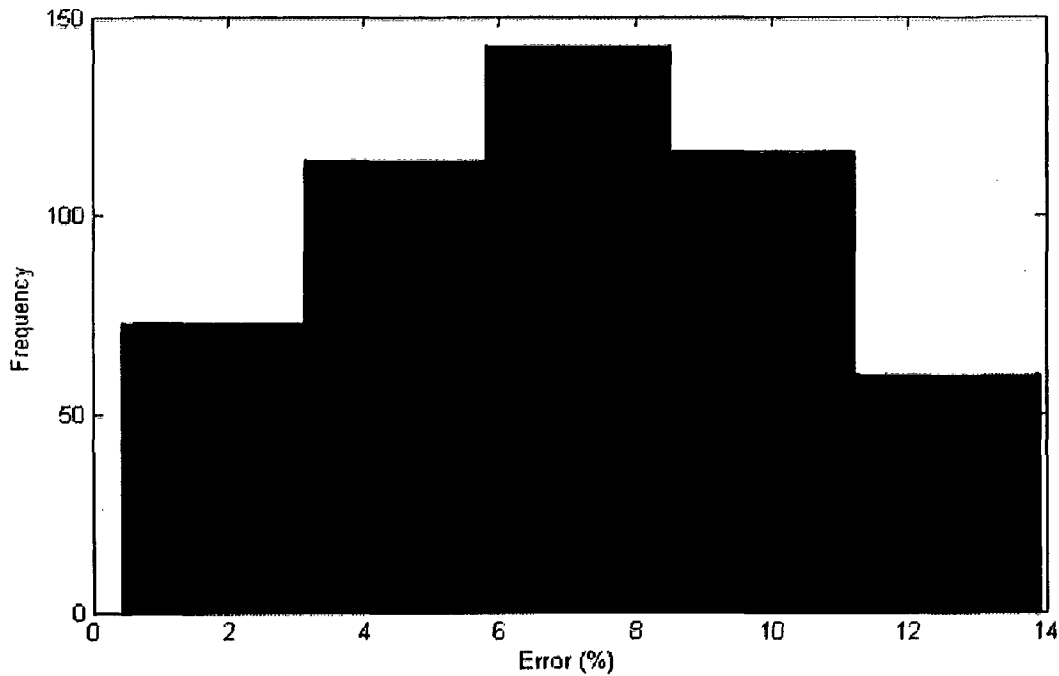


Fig: 27 Histogram showing the frequency against errors.

**Computation of figure of merits:**

Mean squared error (MSE) = 1.8485

Mean absolute error (MAD) = 1.0035

The variation observed for changing various hidden layer neurons is as shown below:

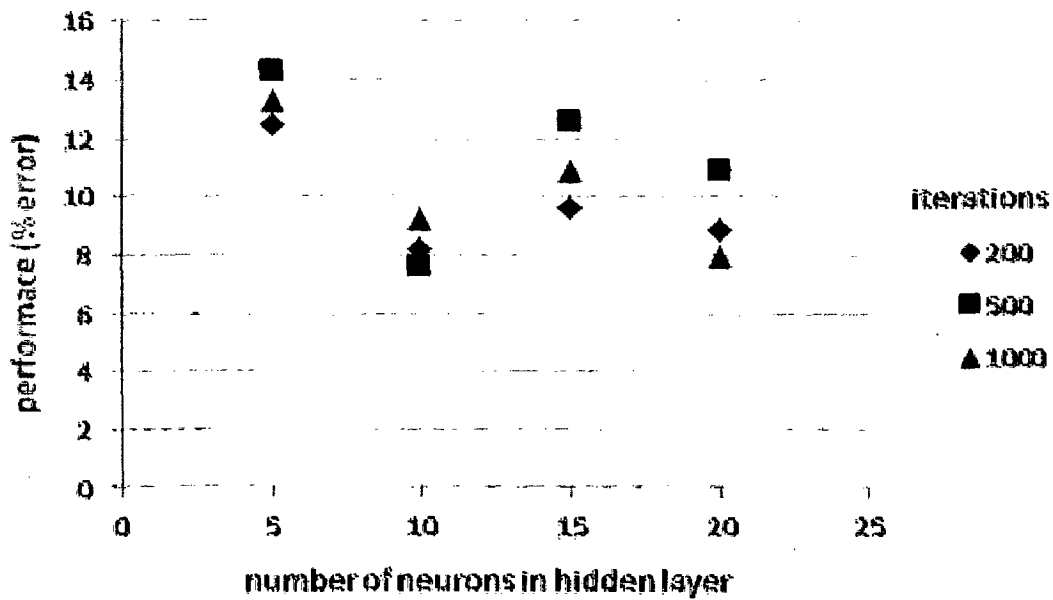


Fig: 28 Comparison of measured and estimated moisture values:

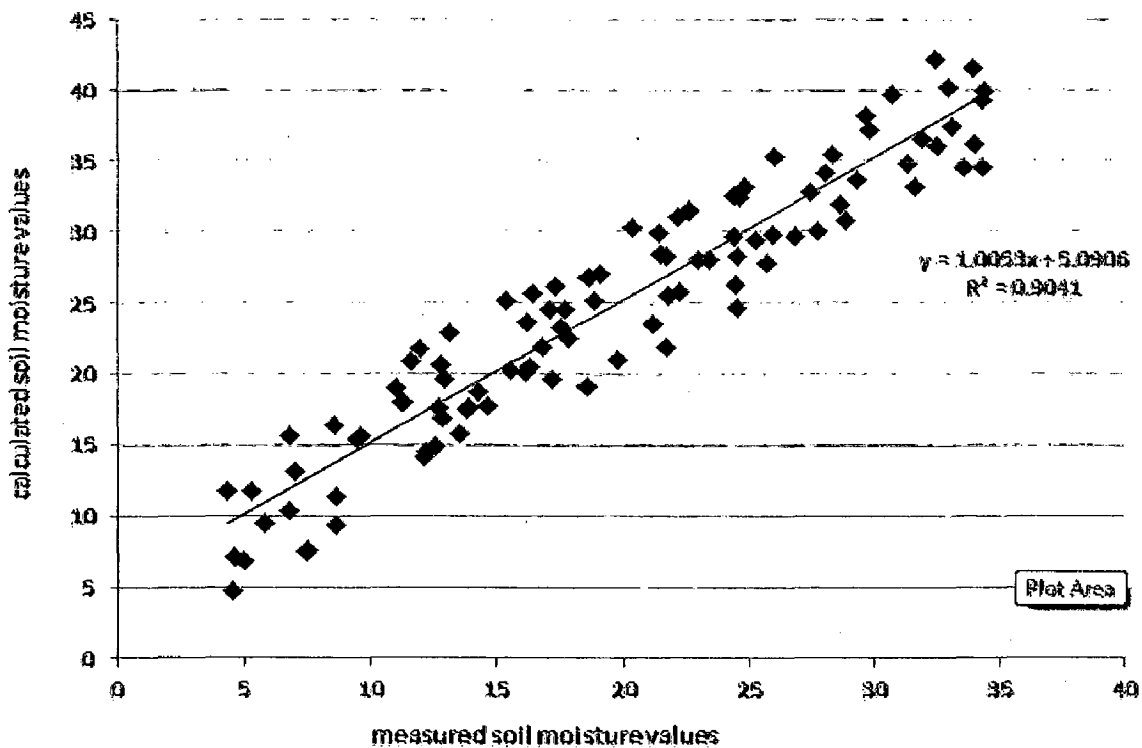


Fig 29: Comparison of predicted and measured moisture values

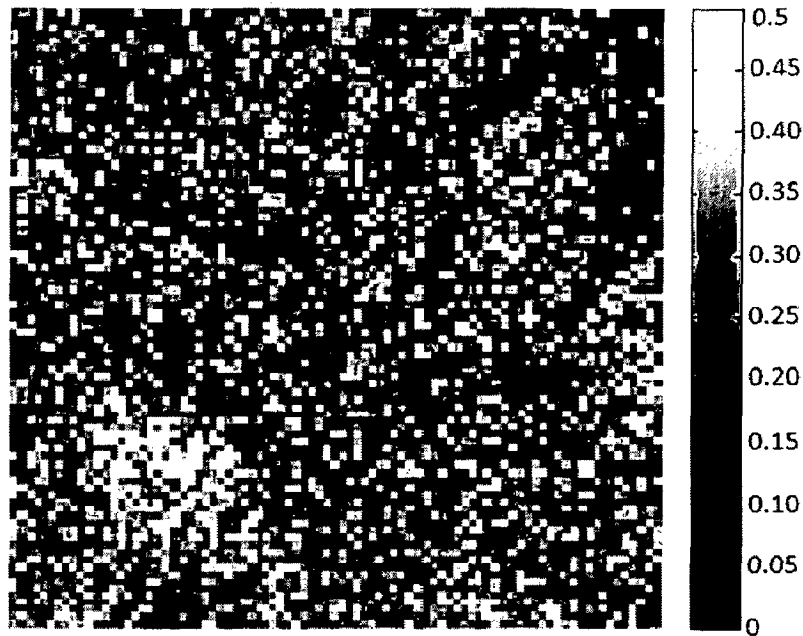


Fig 30: Final moisture map generated by Neural Network Approach

Some salient features of Neural Network are as follows:

- The applying of neural network is done by first normalizing the backscattering values in the range of 0 to 1. This is done for better development of forward model.
- The number of hidden neurons was optimized on trial basis for better training accuracy.
- Adaptive learning mechanism was adopted with a factor of 10% reduction in learning rate when network stucked in local minima.
- Back propagation feed forward algorithm with sigmoid activation function has been used to construct the predictive model.
- The input and output data points were scaled according to the characteristic of sigmoid function.
- A small amount of (0.3) momentum factor has been incorporated to avoid oscillations during training phase.

## 6.4. Nelder Mead Approach

Implementation of Nelder Mead approach

Step 1. First the measured backscattered values from satellite data are obtained both HH and VV

Step 2. A dielectric constant is assumed and corresponding to it the value HH and VV dielectric constant is obtained.

Step 3. A minimization using Nelder Mead method is done between this measure satellite backscattering value and calculated backscattering value.

Step 4. The final value obtained from this minimization is assumed as the corresponding value dielectric constant.

Step 5. From the dielectric constant the moisture value can be calculated by equation

The overall outline of Nelder mead method is shown in Fig 18.

A final comparison is done between the soil moisture value obtained from the Nelder mead method and the measured soil moisture value corresponding to the satellite data obtained from the satellite data HH and VV. This soil moisture from satellite backscattering data HH and VV is obtained from the equation 5.18 and 5.21:

### Result of Nelder Mead approach

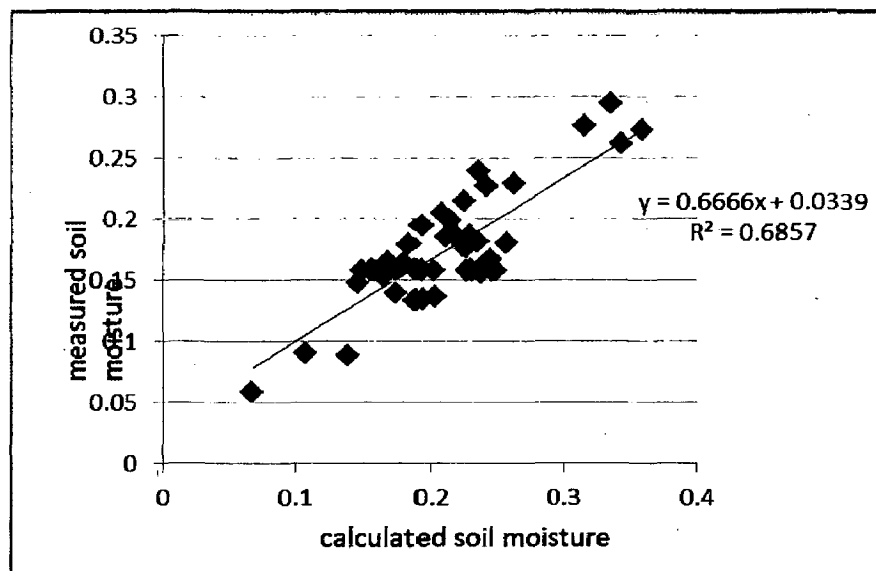


Fig: 31 comparison of result between measured and calculated soil moisture

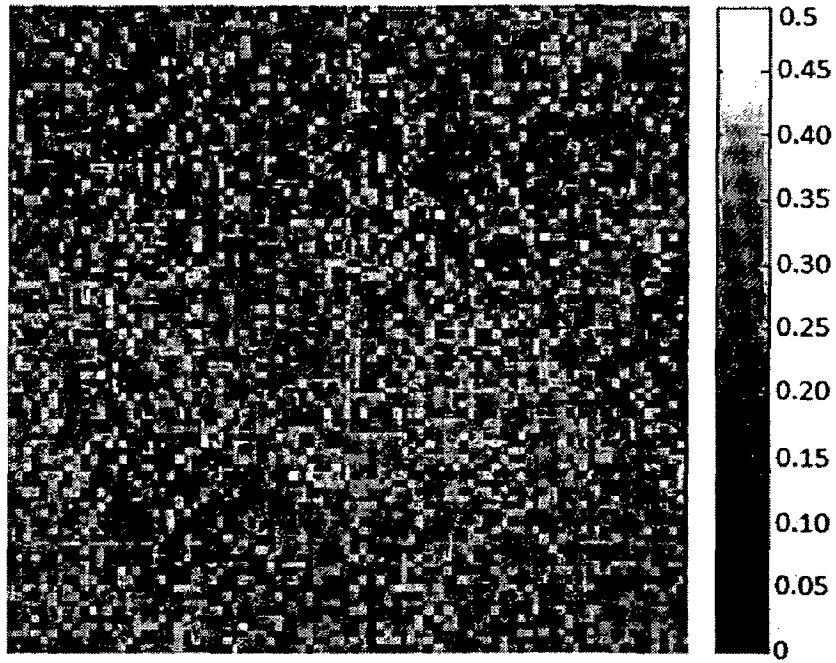


Fig 32: Final moisture map generated by Nelder Mead Approach for same region as in Neural Network





# Chapter 7

## Conclusion and future scope

---

### 7.1. Conclusion

The main objective of this thesis is to develop a model for estimating soil moisture from SAR data and including the factors to normalize the vegetation parameters. This model development has to be adaptive in nature which requires a little a priori knowledge any on site measurement.

In first chapter of this thesis an introduction about the need of soil moisture estimation was mentioned. In next section the overall objective of thesis was defined. The main problem statement of finding a robust and adaptive algorithm for estimating the soil moisture was stated. A brief overview of overall thesis was mentioned.

In second chapter the basics of Microwave remote sensing and a little introduction about active and passive remote sensing was explained. The dependence of soil moisture on satellite parameters as well as topological parameters is explained. The satellite parameters are known to us so the problem finally remains to develop an algorithm dependent on topological factors such as dielectric constant, surface roughness and soil texture etc.

In third chapter a brief review of various theoretical, empirical and semi empirical models which are developed to find out a relation between the soil parameter (soil moisture in this case) and the satellite backscattered data is done. The satellite data is correlated to the dielectric constant of soil from which the moisture values are obtained.

In fourth chapter the details about the study region on which this study of soil moisture is carried out is mentioned. And the corresponding data used is mentioned. Two data are used. First is the polarimetric SAR data (PALSAR) of April 2011. And second is the optical MODIS data of April 2011 is used. MODIS data is basically used for classification of region.

The soil moisture is calculated from the PALSAR data.

In fifth chapter the methodology used for estimating of soil moisture from the SAR data is explained. The main approaches used for estimation of soil moisture from the SAR data are Neural Network, Dubois model for soil moisture estimation and Nelder mead minimization method. The first step is classification of region into different land cover regions as satellite backscattered signal is modified due to the surface topography. The classification of land into various land cover is done using the optical image (MODIS data). The reason for using the optical image for classification is because the image is shows spectrally different behavior to different optical wavelengths. Using this property of land cover various indices are calculated which are can be used to classify the region into land cover regions. Various indices used were NDVI, PAVI, GEMI, PSAVI, and MSAVI. After classification the water and urban regions are masked because the moisture of these regions doesn't mean anything. For the remaining regions the bare soil is separated from vegetated regions. As the vegetation highly effects the satellite backscattering data this vegetation effect has to be normalized with first. For normalizing the vegetation effect the NDVI values are used. After normalizing the vegetation effect, the data is further used for estimating soil moisture. The first technique used for soil moisture estimation is the Neural network. In this approach a feed forward back propagating model is used. In this the two backscattering satellite values HH and VV are used as input and only one output in terms of moisture is taken. First the forward model is developed in which a model is developed between satellite backscattering values and corresponding moisture generated from field visit. After various testing for different combination of hidden layers and corresponding neurons in them, it was observed that one hidden layer with ten neurons gave the best result. After developing the forward model the testing of this model was done for available set of ground truth values. A comparison between the calculated and measured soil moisture values was done using this model. Second model used for classification was Nelder mead model. In Nelder mead model first the satellite values of HH and VV are used. A corresponding dielectric value is assumed from which HH and VV values are calculated. Now a minimization between these two calculated and measured values is done. For this minimized value the corresponding value of dielectric constant is taken as the final value. A comparison is also done for measured and calculated value for a ground truth data set.

In sixth chapter the results of classification as well as moisture estimation are discussed.

Using the different indices of NDVI, GEMI, PAVI, MSAVI, PSAVI a classification of land surface into various land cover classes is done. Classification done using each of these indices is shown separately and finally the common region with all these indices is shown. A comparison of classification using all these indices for four different months is also shown. This classified MODIS image is superimposed on PALSAR image and corresponding water and urban region is masked. For the remaining region containing of bare soil and vegetation, the vegetation effect is normalized using NDVI as a formalizing factor. After normalization the moisture is calculated using Neural network and Nelder Mead approaches. A comparison between the measured and calculated soil moisture is done and finally a moisture map is generated for the same.

## **7.2. Future scope**

- A better classification can be done using more parameters of soil and using even more indices of the soil. Classification of water and urban shows almost similar response to different indices. This problem can be removed by using different bands of MODIS individually and also taking into account more indices.
- Further models can be developed which take topographic variations such as slope into account.  
Including topographic variation is necessary because it greatly affects the estimation of soil moisture because of error it introduces in backscattering coefficient.
- A more robust algorithm is to be studied which takes care of the cloud, smoke and other atmospheric variations.
- Only a single incidence satellite data is used but with two or more incidence angle data a more effective model can be developed which can take into account the shadow effect as well normalize the slope effect of mountainous regions.



## LIST OF PUBLICATION

The following paper has been communicated.

Lokesh Meghwal, Tasneem Ahmed, D.Singh, "Classification of Land cover using different indices on MODIS imagery", IEEE MICROWAVE 2012 conference, July-August, India.



## REFERENCES

- [1]. F. T. Ulaby, "Radar measurements of soil moisture content," IEEE Trans. Antennas Propagation, Vol. AP-22, pp. 257-265, 1974.
- [2]. Lingli WANG, John J. QU, "Satellite remote sensing applications for surface soil moisture monitoring: A review", Front. Earth Sci. China 2009, 3(2): 237–247, 1995
- [3]. R. B. Jackson, I. A. Moore, W. A. Hoffmann, W. T. Pockman, and C. R. Linder, "Ecosystem rooting depth determined with caves and DNA", Vol. 96, pp. 11387–11392, September 1999 Jacobs et al. 2004
- [4]. P. E. O'Neill, N. S. Chauhan & T. J. Jackson, "Use of active and passive microwave remote sensing for soil moisture estimation through corn", Volume 17, Issue 10, pages 1851-1865, 1996
- [5]. Rosnaya et al, "Response of surface energy balance to water regime and vegetation development in a Sahelian landscape", Volume 375, Issues 1–2, 30 August 2009, Pages 178–189;
- [6]. T.J. Schmugge and T.J. Jackson, "observations of coherent emissions from soil", Radio Science, Volume 33, Number 2, page 267-272, March-April 1998 Perspectives on Worldwide Space borne Radar Programs
- [7]. Ulaby, F. R. Moore, and A. Fung, text Microwave remote sensing, active and passive, vol. 3 : {From Theory to Applications}, Dedham, MA, USA, Artech house, (1986) Schmugge and Jackson 1992; Ulaby et al. 1986b
- [8]. Glenn, N. F. and Carr, J. R., 2003. The use of geostatistics in relating soil moisture to RADARSAT-1 SAR data obtained over the Great Basin, Nevada, and USA. Computers & Geosciences, 29 (5) :577-586. van-Zyl 1993
- [9]. E. J. Burke and L. P. Simmonds, "A simple parameterization for retrieving soil moisture from passive microwave data "Hydrology and Earth System Sciences, 5(A1) ,39-48,(2001)
- [10]. F. T. Ulaby, "Inversion problems for passive microwave measurements," IEEE Trans. Antennas Propagation, Vol. AP-22, pp. 257-265, 1974,"

- [11]. Bourgeau-Chavez, L. L., Kasischke, E. S., Riordan, K., Brunzell, S., Nolan, M., Hyer, E., Slawski, J., Medvecz, M., Walters, T. and Ames, S., 2007. Remote monitoring of spatial and temporal surface soil moisture in fire disturbed boreal forest ecosystems with ERS SAR imagery. *International Journal Of Remote Sensing*, 28 (10) :2133-2162
- [12]. Karam, M. A., Fung, A. K., Lang, R. H. and Chauhan, N. S. 1992. 'A microwave scattering model for layered vegetation'. *IEEE Trans. Geosci. Remote Sensing*, GE30(4): 767–784
- [13]. McDonald, K. C. and Ulaby, F. T. 1993. 'Radiative transfer modeling of discontinuous tree canopies at microwave frequencies'. *Int. J. Remote Sens.*, 14(11): 2097–2128. [Taylor & Francis Online], [Web of Science ®], [CSA]
- [14]. Bindlish, R. and Barros, A. P., 2000. Multifrequency soil moisture inversion from SAR measurements with the use of IEM. *Remote Sensing Of Environment*, 71 (1):67-88.
- [15]. J.szilagyi, D.C.Rundquist, and D.C.Gosselin,"NDVI relationship to monthly evaporation", *Geophysical Research letters*, vol.25, No.10, pages-1753-1756, May,1998
- [16]. Quan Wang, Samuel Adiku, John Tenhunen, Andre' Granier, "On the relationship of NDVI with leaf area index in a deciduous forest site ", *Remote Sensing of Environment* 94 (2005) 244–255
- [17]. Karam, M. A., Fung, A. K., Lang, R. H. and Chauhan, N. S. 1992. 'A microwave scattering model for layered vegetation'. *IEEE Trans. Geosci. Remote Sensing*, GE30(4): 767–784
- [18]. Oh, Y., Sarabandi, K., and Ulaby, F. T.: An empirical model and an inversion technique for radar scattering from bare soil surfaces, *IEEE T. Geosci. Remote Sens.*, 30, 370–381, 1992.
- [19]. Wang, J. R., Hsu, A., Shi, J. C., O'Neill, P. E., and Engman, E. T.: A comparison of soil moisture retrieval models using SIR-C measurements over the Little Washita River watershed, *Remote Sens. Environ.*, 59, 308–320, 1997.
- [20]. Fung, A. K., Li, Z., and Chen, K. S.: Backscattering from a randomly rough dielectric surface, *IEEE Geosci. Remote Sens.*, 30, 356–369, 1992.



- [21]. Baghdadi, N., King, C., Chanzy, A., and Wigneron, J. P.: An empirical calibration of the Integral Equation Model based on SAR data, soil moisture and surface roughness measurement over bare soils, *Int. J. Remote Sens.*, 23, 4325–4340, 2002.
- [22]. Zribi, M. and Dechambre, M. A.: A new empirical model to retrieve soil moisture and roughness from radar data, *Remote Sens. Environ.*, 84, 42–52, 2002.
- [23]. Pascale C. Dubois and Jakob van Zyl, "An empirical soil moisture estimation algorithm using imaging radar "Jet Propulsion Laboratory, California Institute of Technology, 1994
- [24]. Karam et al, "The Potential Of Microwave Radiometers In Monitoring Forest Biomass", Aerojet Electronic System Plant, 1860-1863
- [25]. Nicolas Baghdadi, Elie Saba, Maelle Aubert, Mehrez Zribi, and Frederic Baup, "Evaluation of Radar Backscattering Models IEM, Oh, and Dubois for SAR Data in X-Band Over Bare Soils"
- [26]. Urška Demšar, "A strategy for observing soil moisture by remote sensing in the Murray-Darling basin", Department of Infrastructure, Royal Institute of Technology (KTH), 2005
- [27]. M. Shoshany et al. "The relationship between ERS-2 SAR backscatter and soil moisture: generalization from a humid to semi-arid transect "Department of Geography, Bar-Ilan University, Ramat-Gan 52900, Israel, *int. j. remote sensing*, 2000, vol. 21, no. 11, 2337–2343
- [28]. Claude R. Duguay, "Estimating Vapor-transpiration within the Colorado Alpine Tundra with Land SAT Thematic Mapper, "Estimating Evapo-transpiration within the Colorado Alpine Tundra with LandsAT Thematic Mapper Laboratory for Earth Observation and Information Systems, Department of Geography, University of Ottawa, Canada
- [29]. M. Susan Moran, Stephen McElroy, Joseph M. Watts, and Christa D. Peters-Lidard, "Radar Remote Sensing for Estimation of Surface Soil Moisture at the Watershed Scale", 2005 by Texas A&M
- [30]. Joseph F. Knight1 et al, "Regional Scale Land Cover Characterization using MODIS NDVI 250 m Multi-Temporal Imagery: A Phenology-Based Approach", Center for Earth Observation, North Carolina State University, Raleigh, NC 27695-7106, USA

- [31]. D. Singh, E.F. Silva, J.P. Berroir, I. Herlin, G.A. Costa, M.S.P. Meirelles, "Environmental degradation analysis using NOAA/AVHRR data" *Advances in Space Research*.
- [32]. Xiumin Zhang; Zhuotong Nan; Yu Sheng; Lin Zhao; Jichun Wu; Guoying Zhou, "A new method of vegetation classification based on temporal distribution of vegetation indices", *Remote Sensing, Environment and Transportation Engineering (RSETE)*, 2011 International Conference on 24-26 June 2011, pages:13 – 16
- [33]. Yuliang, Q., Yun, Q. Fast soil erosion investigation and dynamic analysis in the loess plateau of China by using information composite technique. *Advances in Space Research* 29 (No. 1), 85–88, 2002.
- [34]. Zhang Chunsen, "Extraction of the Vegetation Information Based on Temporal and Spectrum Information", *Coll. of Geometrics, Xi'an Univ. of Sci. & Technol., Xi'an, China*, 29-31 Oct. 2010, On Page(s): 1 – 4
- [35]. R.Prakash, D.Singh, "A Fusion Approach to Retrieve Soil Moisture With SAR and Optical Data", *Dept. of Electron. & Computer Eng., Indian Inst. of Technol. Roorkee, Roorkee, India* Volume: 5, Issue: 1, On Page(s): 196 – 206
- [36]. M. Angiulli, C. Notarnicola, F.Posa, P.Pampaloni, "L-band active-passive and L-C-X-bands passive data for soil moisture retrieval, two different approaches in comparison", *Geoscience and Remote Sensing Symposium, 2004. IGARSS '04. Proceedings. 2004 IEEE International*, Pages 4492-4495
- [37]. Claudia Notarnicola and Francesco Posa, "Bayesian Algorithm for the Estimation of the Dielectric Constant from Active and Passive Remotely Sensed Data", *IEEE Geoscience and remote sensing letters*, Vol. 1, No. 3 pages:179-183, July 2004,
- [38]. Claudia Notarnicola and Francesco Posa, "Inferring Vegetation Water Content From C- and L-Band SAR Images", *IEEE Transactions on Geoscience and remote sensing*, vol. 45, No. 10, pages: 3165-3171
- [39]. Jeff Settle, "On the Use of Remotely Sensed Data to Estimate Spatially Averaged Geophysical Variables", *IEEE Transactions on Geoscience and remote sensing*, vol. 42, No. 3, March 2004, pages: 620-631

- [40]. Claudia Notarnicola, Mariella Angiulli, and Francesco Posa, "Use of Radar and Optical Remotely Sensed Data for Soil Moisture Retrieval Over Vegetated Areas" *IEEE Transactions on geoscience and remote sensing*, Vol. 44, No. 4, April 2006,
- [41]. Simonetta Paloscia and Simone Pettinato, "A Comparison of Algorithms for Retrieving Soil Moisture from ENVISAT/ASAR Images", *IEEE transactions on Geoscience and remote sensing*, vol. 46, no. 10, October 2008, pages:3274-3284
- [42]. Notarnicola, Claudia, "Group Inversion Approach" for Detection of Soil Moisture Temporal-Invariant Locations", *Remote Sensing*, vol. 1, issue 4, pp. 1338-1352, 2009
- [43]. Prakash, R.; Singh, D.; Pathak, N.P., "A Fusion Approach to Retrieve Soil Moisture With SAR and Optical Data", *Selected Topics in Applied Earth Observations and Remote Sensing*, *IEEE Journal of Geoscience & Remote Sensing Society*, Feb. 2012, Volume: 5 , Issue: 1, Page(s): 196-206
- [44]. P. Mishra and D. Singh, "land cover classification of PALSAR images by knowledge based decision tree classifier and supervised classifiers based on SAR observables", *Progress In Electromagnetics Research B*, Vol. 30, 47–70, 2011
- [45]. Wang, C., Qi, J., Moran, S. and Marsett, R., 2004, Soil moisture estimation in a semiarid range land using ERS–2 and TM imagery. *Remote Sensing of Environment*, **90**, pp. 178–189.
- [46]. Myneni, R.B., Hall, F.G., Sellers, P.J. and Marshak, A.L., 1995, "The interpretation of spectral vegetation indexes. *IEEE Transactions on Geoscience and Remote Sensing*, **33**, pp. 481–486.
- [47]. Allen, C. T., Ulaby, F. T., and Fung, A. F.(1982), A model for the radar backscattering coefficient of bare soft, University of Kansas Center for Research, Inc., Lawrence, RSL TR 460-8 (AgRISTARS SM-K1-04181).
- [48]. Ulaby, F.T., Dubois, P.C. & Van Zyl, J. (1996): Radar Mapping of Surface Soil Moisture, *Journal of Hydrology*, **184**, 57-84.
- [49]. A. Michelle Wood and Nelson D. Sherry, "Mixing of chlorophyll from the Middle Atlantic Bight cold pool into the Gulf Stream at Cape Hatteras in July 1993", *Journal of Geophysical research*, Vol. 101, no. C9, pages 579-593, September 15, 1996

- [50]. Eric S. Kasischke, Mihai A. Tanase, Laura L. Bourgeau-Chavez, Matthew Borr, "Soil moisture limitations on monitoring boreal forest regrowth using spaceborne L-band SAR data", *Remote Sensing of Environment* 115 (2011) 227–232
- [51]. Qi, J., Chehbouni, A., Huete, A.R., Kerr, Y.H. and Sorooshian, S. 1994. A modified soil adjusted vegetation index. *Remote Sens. Environ.* 48, 119-126
- [52]. Pinty, B., and M. M. Verstraete, "GEMI: A non-linear index to monitor global vegetation from satellites, *Vegetation*, 101, 15-20, 1992
- [53]. Bunkei Matsushita, Wei Yang, Jin Chen, Yuyichi Onda and Guoyu Qiu, "Sensitivity of the Enhanced Vegetation Index (EVI) and Normalized Difference Vegetation Index (NDVI) to Topographic Effects: A Case Study in High-Density Cypress Forest", *Sensors* 2007, 7, 2636-2651
- [54]. Y. Zha, Y.Gao, S. Ni, Use of normalized difference built-up index in automatically mapping urban areas from TM imagery. *Int.J. Remote Sensing*, 24(3), pp. 583-594, 2003.
- [55]. M. S. Meirelles, G. A. Costa, D. Singh, J. P. Berroir, I. Herlin, E. F. Silva, H. L. Coutinho, "A methodology to support the analysis of environmental degradation using NOAA AVHRR data"
- [56]. Rahman, M.M., M.S. Moran, D.P. Thoma, R. Bryant, E.E. Sano, C.D. Holifield-Collins, S. Skirvin, C. Kershner and B. J. Orr, A derivation of roughness correlation length for parameterizing radar backscatter models, *Intl. J. Rem. Sens.* August 2005.